

**Schlumberger, Sugar Land Campus**

**Numerical Simulation of 3D DC and AC Resistivity Logging  
Measurements in Deviated Wells Using a Fourier Series  
Expansion in a Non-Orthogonal System of Coordinates**

**D. Pardo, M. J. Nam, C. Torres-Verdín, M. Paszynski, V. M. Calo**

**hp-FE TEAM: D. Pardo, M. Paszynski, M. J. Nam, Ch. Michler,  
R. Abdollah-Pour, L. Demkowicz, C. Torres-Verdín**

**September 19, 2007**



**Department of Petroleum and Geosystems Engineering**

**THE UNIVERSITY OF TEXAS AT AUSTIN**

# OVERVIEW

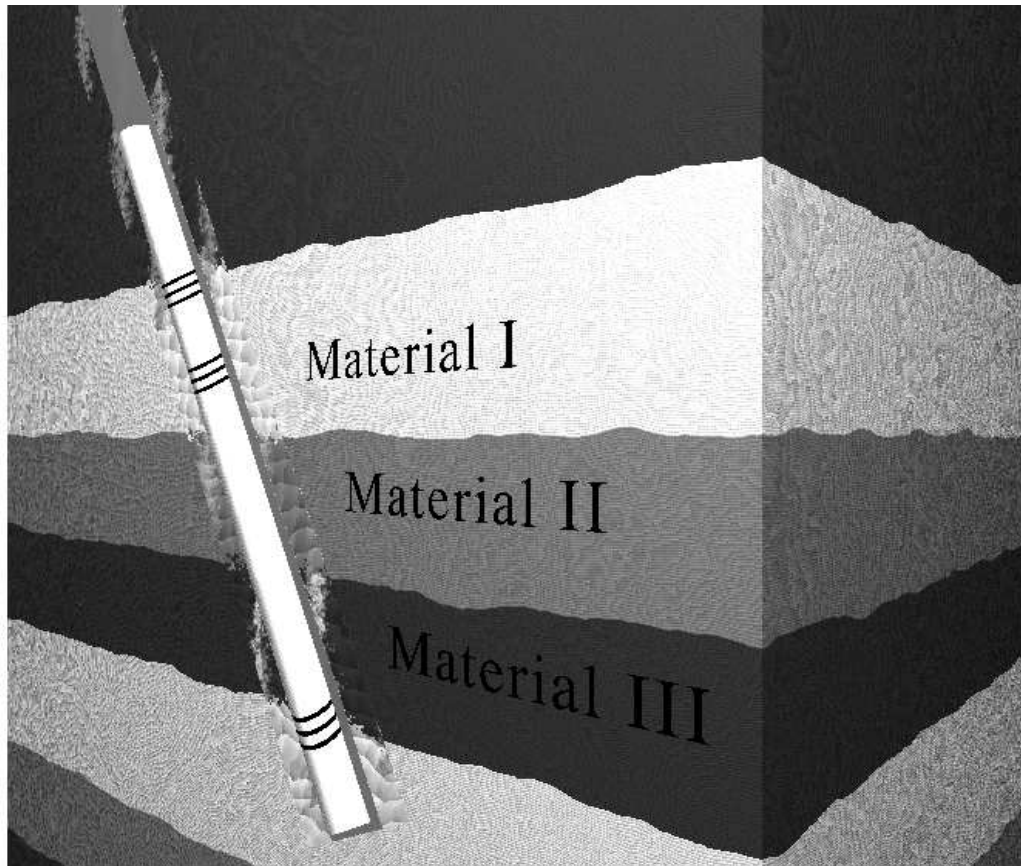
---

1. **Motivation: Simulation of resistivity logging measurements in deviated wells.**
2. **Methodology:**
  - Fourier series expansion.
  - Non-orthogonal system of coordinates.
  - 2D goal-oriented self-adaptive  $hp$ -FEM.
  - Verification of the methodology.
3. **Numerical results:**
  - 3D DC through-casing measurements in deviated wells.
  - 3D DC dual laterolog measurements in deviated wells.
  - 3D AC wireline and LWD measurements in deviated wells.
4. **Conclusions and future work.**

# MOTIVATION (APPLICATIONS)

---

## Deviated Wells (Forward Problem)



Dip Angle  
Invasion  
Anisotropy  
Triaxial Induction  
Eccentricity  
Laterolog  
Through-Casing  
Induction-LWD  
Induction-Wireline  
Inverse Problems  
Multi-Physics

**Objective: Find solution at the receiver antennas.**

## MOTIVATION (APPLICATIONS)

### 3D Variational Formulation

#### Time-Harmonic Maxwell's Equations

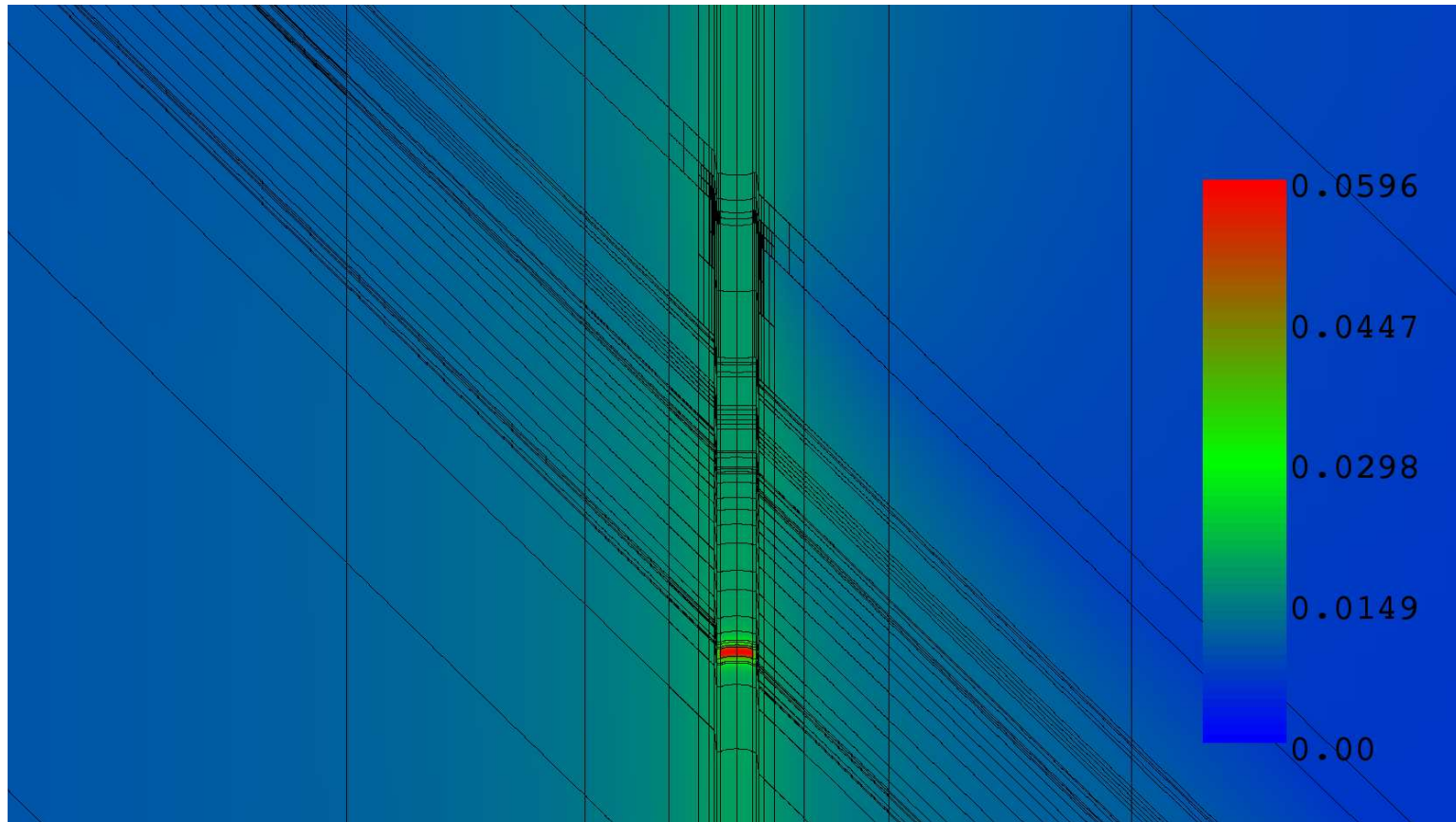
$\nabla \times \mathbf{H} = (\bar{\sigma} + j\omega\bar{\epsilon})\mathbf{E} + \mathbf{J}^{imp}$	<b>Ampere's law</b>
$\nabla \times \mathbf{E} = -j\omega\bar{\mu}\mathbf{H} - \mathbf{M}^{imp}$	<b>Faraday's law</b>
$\nabla \cdot (\bar{\epsilon}\mathbf{E}) = \rho$	<b>Gauss' law of Electricity</b>
$\nabla \cdot (\bar{\mu}\mathbf{H}) = 0$	<b>Gauss' law of Magnetism</b>

#### E-VARIATIONAL FORMULATION:

$$\left\{ \begin{array}{l} \text{Find } \mathbf{E} \in \mathbf{E}_D + \mathbf{H}_D(\text{curl}; \Omega) \text{ such that:} \\ \int_{\Omega} (\bar{\mu}^{-1} \nabla \times \mathbf{E}) \cdot (\nabla \times \bar{\mathbf{F}}) dV - \int_{\Omega} (\bar{k}^2 \mathbf{E}) \cdot \bar{\mathbf{F}} dV = -j\omega \int_{\Omega} \mathbf{J}^{imp} \cdot \bar{\mathbf{F}} dV \\ + j\omega \int_{\Gamma_N} \mathbf{J}_{\Gamma_N}^{imp} \cdot \bar{\mathbf{F}}_t dS - \int_{\Omega} (\bar{\mu}^{-1} \mathbf{M}^{imp}) \cdot (\nabla \times \bar{\mathbf{F}}) dV \quad \forall \bar{\mathbf{F}} \in \mathbf{H}_D(\text{curl}; \Omega) \end{array} \right.$$

## MOTIVATION (APPLICATIONS)

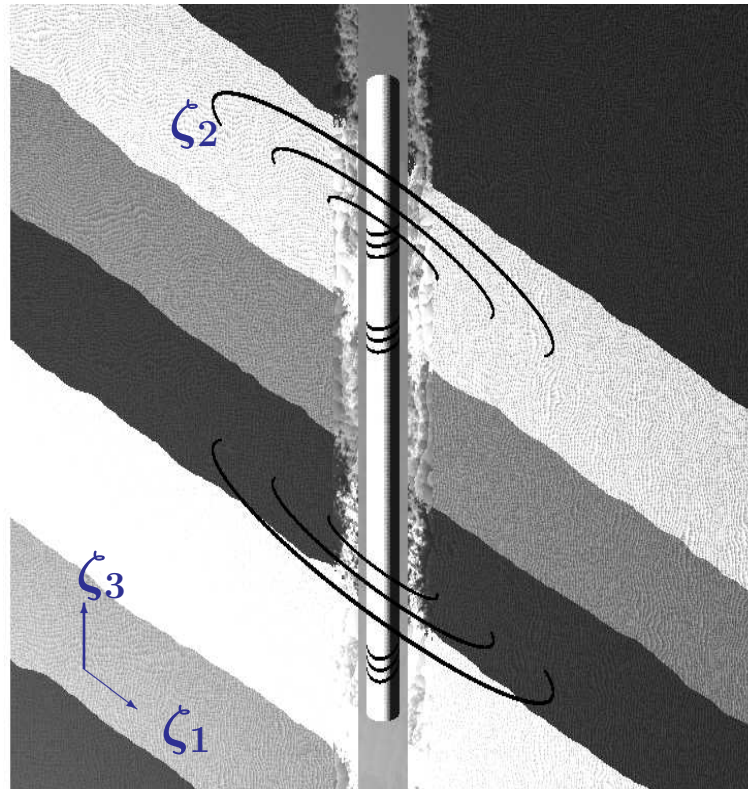
Example: Solution in a 60-degree deviated well ( $-\nabla\sigma\nabla u = f$ )



Several hours to obtain one solution (3D forward simulation).  
Several months needed to solve the inverse problem.

## METHODOLOGY: MAIN IDEA

### Non-Orthogonal System of Coordinates



Material coefficients are constant with respect to the quasi-azimuthal direction  $\zeta_2$

### Fourier Series Expansion in $\zeta_2$

DC Problems:  $-\nabla \sigma \nabla u = f$

$$u(\zeta_1, \zeta_2, \zeta_3) = \sum_{l=-\infty}^{l=\infty} u_l(\zeta_1, \zeta_3) e^{jl\zeta_2}$$

$$\sigma(\zeta_1, \zeta_2, \zeta_3) = \sum_{m=-\infty}^{m=\infty} \sigma_m(\zeta_1, \zeta_3) e^{jm\zeta_2}$$

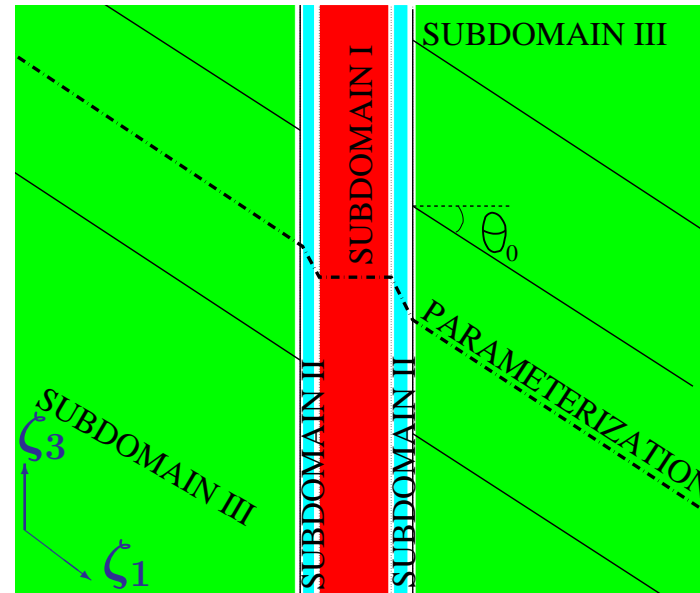
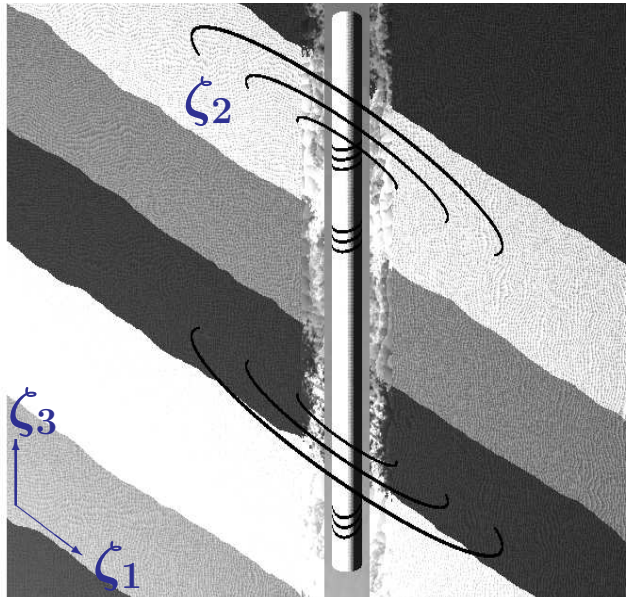
$$f(\zeta_1, \zeta_2, \zeta_3) = \sum_{n=-\infty}^{n=\infty} f_n(\zeta_1, \zeta_3) e^{jn\zeta_2}$$

Fourier modes  $e^{jl\zeta_2}$  are orthogonal high-order basis functions that are (almost) invariant with respect to the gradient operator.

# METHODOLOGY: NEW SYSTEM OF COORDINATES

Cartesian system of coordinates:  $\mathbf{x} = (x_1, x_2, x_3)$ .

New non-orthogonal system of coordinates:  $\zeta = (\zeta_1, \zeta_2, \zeta_3)$ .



**Subdomain I**

;

**Subdomain II**

;

**Subdomain III**

$$\begin{cases} x_1 = \zeta_1 \cos \zeta_2 \\ x_2 = \zeta_1 \sin \zeta_2 \\ x_3 = \zeta_3 \end{cases}$$

$$\begin{cases} x_1 = \zeta_1 \cos \zeta_2 \\ x_2 = \zeta_1 \sin \zeta_2 \\ x_3 = \zeta_3 + \tan \theta_0 \frac{\zeta_1 - \rho_1}{\rho_2 - \rho_1} \rho_2 \end{cases}$$

$$\begin{cases} x_1 = \zeta_1 \cos \zeta_2 \\ x_2 = \zeta_1 \sin \zeta_2 \\ x_3 = \zeta_3 + \tan \theta_0 \zeta_1 \end{cases}$$

# METHODOLOGY: NEW SYSTEM OF COORDINATES

## Final Variational Formulation

We define the Jacobian matrix  $\mathcal{J} = \frac{\partial(x_1, x_2, x_3)}{\partial(\zeta_1, \zeta_2, \zeta_3)}$  and its determinant  $|\mathcal{J}| = \det(\mathcal{J})$ .

Variational formulation in the new system of coordinates:

$$\left\{ \begin{array}{l} \text{Find } u \in u_D + H_D^1(\Omega) \text{ such that:} \\ \left\langle \frac{\partial v}{\partial \zeta}, \tilde{\sigma} \frac{\partial u}{\partial \zeta} \right\rangle_{L^2(\Omega)} = \left\langle v, \tilde{f} \right\rangle_{L^2(\Omega)} \quad \forall v \in H_D^1(\Omega), \end{array} \right.$$

where:

$$\tilde{\sigma} := \mathcal{J}^{-1} \sigma \mathcal{J}^{-1T} |\mathcal{J}| \quad ; \quad \tilde{f} := f |\mathcal{J}| .$$

**Same variational formulation with new materials and load data**



## METHODOLOGY: FOURIER SERIES EXPANSION

---

For a mono-modal test function  $v = v_k e^{jk\zeta_2}$ , we have:

$$\left\{ \begin{array}{l} \text{Find } u \in u_D + H_D^1(\Omega) \text{ such that:} \\ \sum_{m,n} \left\langle \left( \frac{\partial v}{\partial \zeta} \right)_k e^{jk\zeta_2}, \tilde{\sigma}_m \left( \frac{\partial u}{\partial \zeta} \right)_n e^{j(m+n)\zeta_2} \right\rangle_{L^2(\Omega)} = \\ = \sum_l \left\langle v_k e^{jk\zeta_2}, \tilde{f}_l e^{jl\zeta_2} \right\rangle_{L^2(\Omega)} \quad \forall v_k e^{jk\zeta_2} \in H_D^1(\Omega) \end{array} \right.$$

Using the  $L^2$ -orthogonality of Fourier modes:

$$\left\{ \begin{array}{l} \text{Find } u \in u_D + H_D^1(\Omega) \text{ such that:} \\ \sum_n \left\langle \left( \frac{\partial v}{\partial \zeta} \right)_k, \tilde{\sigma}_{k-n} \left( \frac{\partial u}{\partial \zeta} \right)_n \right\rangle_{L^2(\Omega_{2D})} = \left\langle v_k, \tilde{f}_k \right\rangle_{L^2(\Omega_{2D})} \quad \forall v_k \end{array} \right.$$

## METHODOLOGY: FOURIER SERIES EXPANSION

---

Five Fourier modes are enough to represent EXACTLY the new material coefficients.

$$\tilde{\sigma}(\zeta_1, \zeta_2, \zeta_3) = \sum_{m=-2}^{m=2} \tilde{\sigma}_m(\zeta_1, \zeta_3) e^{jm\zeta_2}$$

## METHODOLOGY: FOURIER SERIES EXPANSION

---

Five Fourier modes are enough to represent EXACTLY the new material coefficients.

$$\tilde{\sigma}(\zeta_1, \zeta_2, \zeta_3) = \sum_{m=-2}^{m=2} \tilde{\sigma}_m(\zeta_1, \zeta_3) e^{jm\zeta_2}$$


---

### Final Variational Formulation

$$\left\{ \begin{array}{l} \text{Find } u \in u_D + H_D^1(\Omega) \text{ such that:} \\ \sum_{n=k-2}^{n=k+2} \left\langle \left( \frac{\partial v}{\partial \zeta} \right)_k, \tilde{\sigma}_{k-n} \left( \frac{\partial u}{\partial \zeta} \right)_n \right\rangle_{L^2(\Omega_{2D})} = \left\langle v_k, \tilde{f}_k \right\rangle_{L^2(\Omega_{2D})} \quad \forall v_k \end{array} \right.$$

## METHODOLOGY: VARIATIONAL FORMULATION

---

Five Fourier modes are enough to represent EXACTLY the new material coefficients.

### Direct Current:

$$\left\{ \begin{array}{l} \text{Find } u \in u_D + H_D^1(\Omega) \text{ such that:} \\ \sum_{n=k-2}^{n=k+2} \left\langle \left( \frac{\partial v}{\partial \zeta} \right)_k, \tilde{\sigma}_{k-n} \left( \frac{\partial u}{\partial \zeta} \right)_n \right\rangle_{L^2(\Omega_{2D})} = \left\langle v_k, \tilde{f}_k \right\rangle_{L^2(\Omega_{2D})} \quad \forall v_k \end{array} \right.$$

### Alternate Current:

$$\left\{ \begin{array}{l} \text{Find } (\mathbf{E})_s \in H_{\Gamma_E}(\text{curl}; \Omega) \text{ such that:} \\ \sum_{n=s-2}^{n=s+2} \left\langle (\nabla^\zeta \times \mathbf{F})_s, (\tilde{\mu}^{-1})_{s-n} (\nabla^\zeta \times \mathbf{E})_l \right\rangle_{L^2(\Omega_{2D})} \\ - \left\langle \mathbf{F}_s, (\tilde{k}^2)_{s-n} \mathbf{E}_l \right\rangle_{L^2(\Omega_{2D})} = -j\omega \left\langle \mathbf{F}_s, (\tilde{\mathbf{J}}^{imp})_s \right\rangle_{L^2(\Omega_{2D})} \quad \forall \mathbf{F}_s \end{array} \right.$$

# METHODOLOGY: IMPLEMENTATION

## Example (7 Fourier Modes)

$$\sum_{n=k-2}^{n=k+2} \underbrace{\left\langle \left( \frac{\partial v}{\partial \zeta} \right)_k, \tilde{\sigma}_{k-n} \left( \frac{\partial u}{\partial \zeta} \right)_n \right\rangle_{L^2(\Omega_{2D})}}_{(k, k-n, n)} = \left\langle v_k, \tilde{f}_k \right\rangle_{L^2(\Omega_{2D})}$$

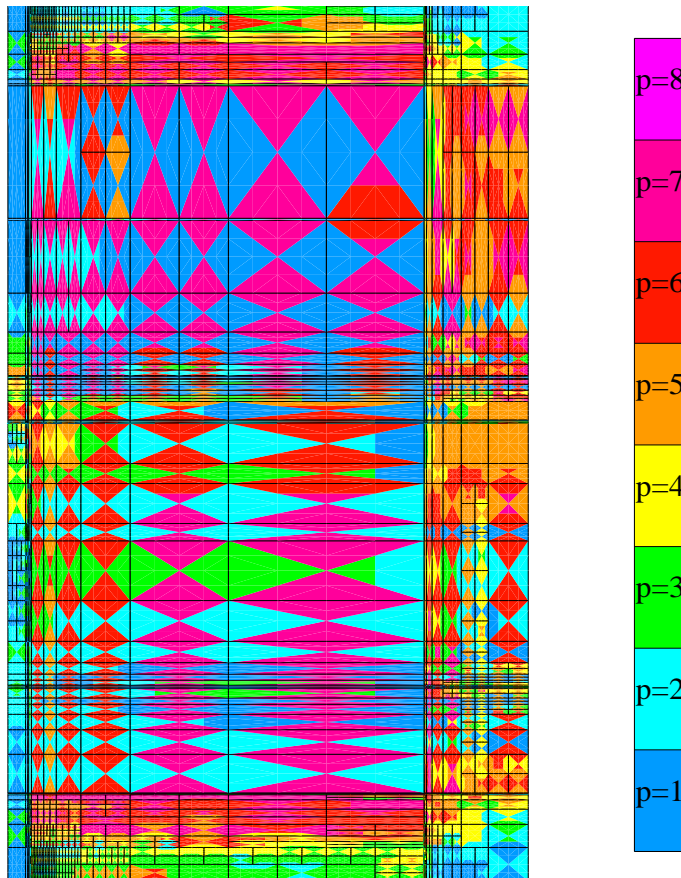
**Stiffness Matrix:**

$$\begin{pmatrix} (-3,0,-3) & (-3,-1,-2) & (-3,-2,-1) & 0 & 0 & 0 & 0 \\ (-2,1,-3) & (-2,0,-2) & (-2,-1,-1) & (-2,-2,0) & 0 & 0 & 0 \\ (-1,2,-3) & (-1,1,-2) & (-1,0,-1) & (-1,-1,0) & (-1,-2,1) & 0 & 0 \\ 0 & (0,2,-2) & (0,1,-1) & (0,0,0) & (0,-1,1) & (0,-2,2) & 0 \\ 0 & 0 & (1,2,-1) & (1,1,0) & (1,0,1) & (1,-1,2) & (1,-2,3) \\ 0 & 0 & 0 & (2,2,0) & (2,1,1) & (2,0,2) & (2,-1,3) \\ 0 & 0 & 0 & 0 & (3,2,1) & (3,1,2) & (3,0,3) \end{pmatrix}$$

## METHODOLOGY: 2D $hp$ -FEM

### A Self-Adaptive Goal-Oriented $hp$ -FEM

Optimal 2D Grid  
(Through Casing Resistivity Problem)



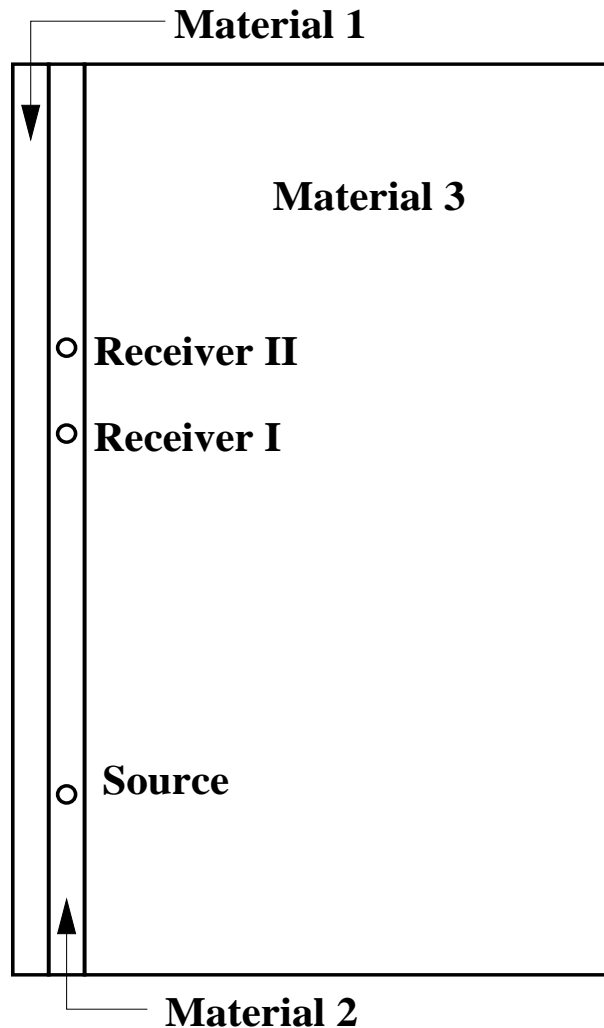
We vary locally the element size  $h$  and the polynomial order of approximation  $p$  throughout the grid.

Optimal grids are **automatically generated** by the computer.

The self-adaptive goal-oriented  $hp$ -FEM provides **exponential convergence** rates in terms of the CPU time vs. the error in a user prescribed quantity of interest.

# NUMERICAL RESULTS: VERIFICATION

## Three Model Problems



### Problem I (Uniform Materials)

Material 1:  $1 \Omega\text{-m}$

Material 2:  $1 \Omega\text{-m}$

Material 3:  $1 \Omega\text{-m}$

### Problem II

Material 1:  $0.00001 \Omega\text{-m}$

Material 2:  $10 \Omega\text{-m}$

Material 3:  $1 \Omega\text{-m}$

### Problem III

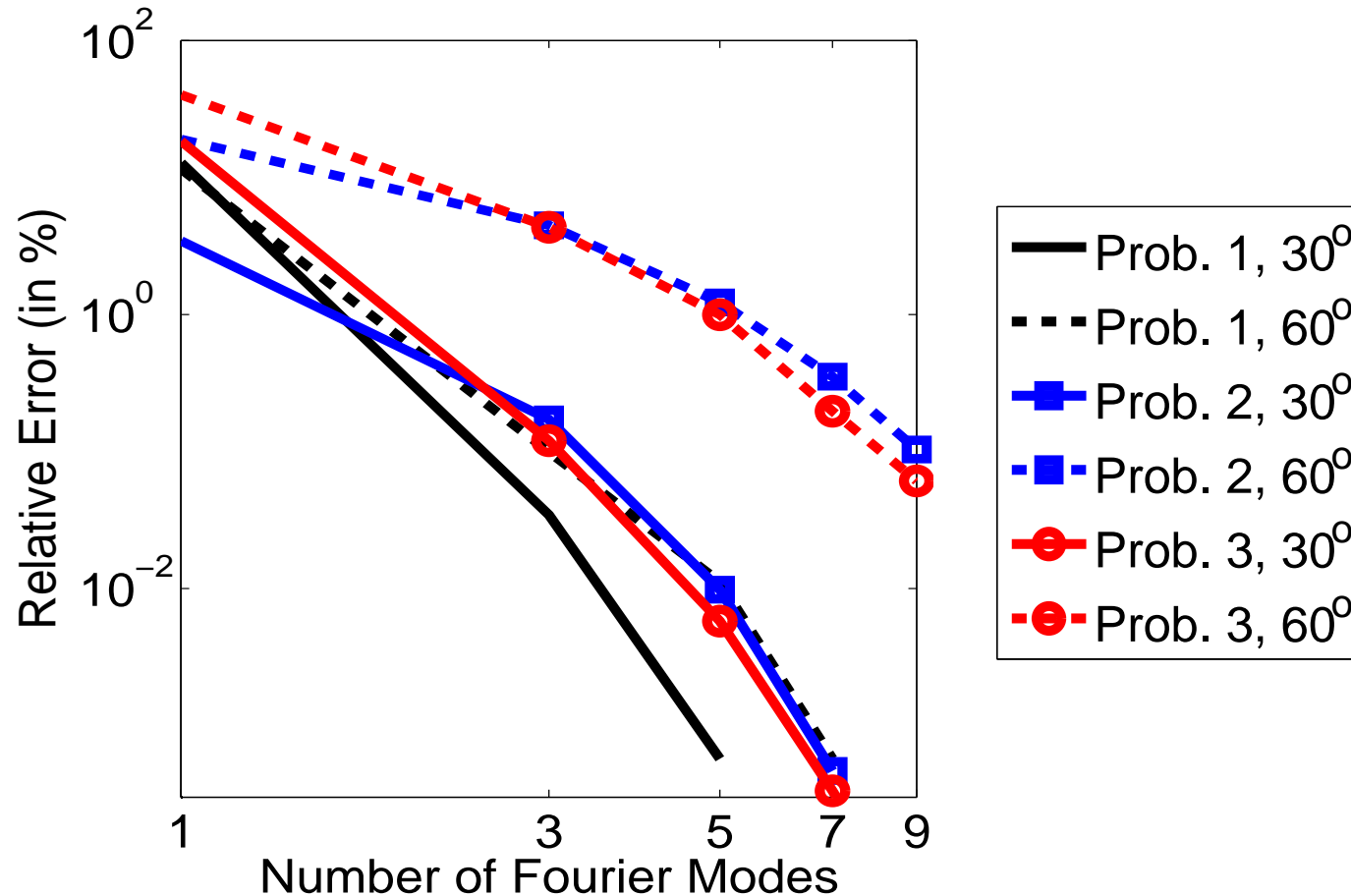
Material 1:  $10000 \Omega\text{-m}$

Material 2:  $0.2 \Omega\text{-m}$

Material 3:  $1 \Omega\text{-m}$

# NUMERICAL RESULTS: VERIFICATION

## Three Model Problems (DC)



**Exponential Convergence in terms of the Number of Fourier Modes**

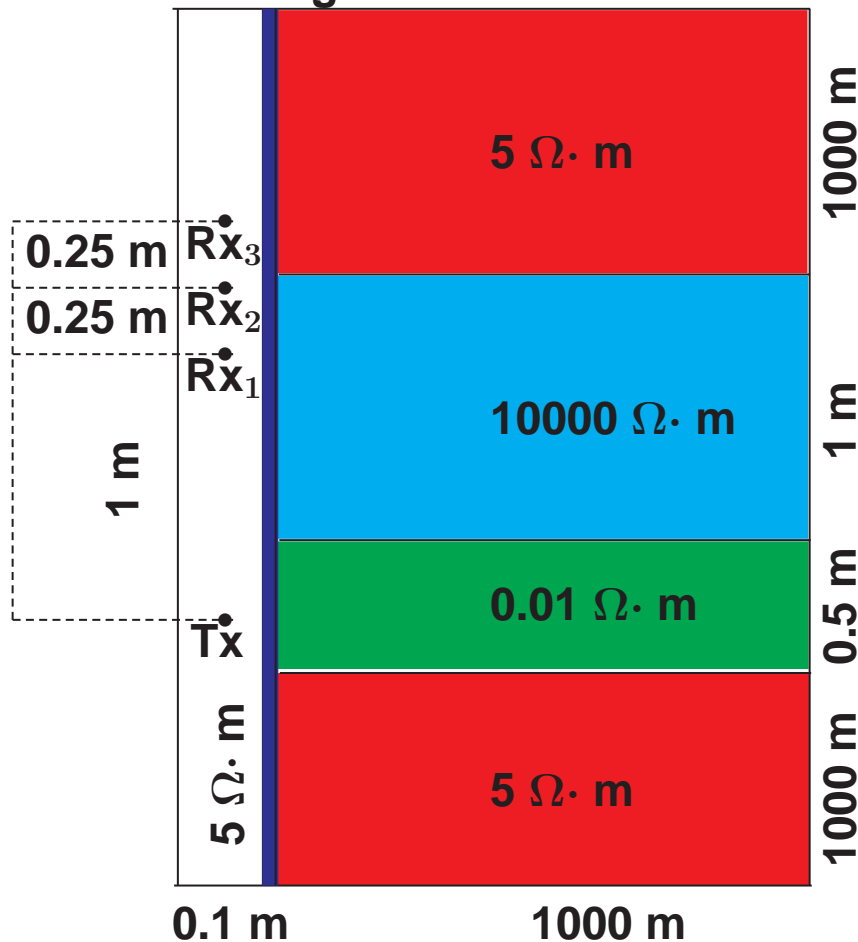


# NUMERICAL RESULTS: DC RESULTS

## Simulation of Through Casing Resistivity Measurements

Casing resistivity:  $10^{-5} - 10^{-7} \Omega \cdot m$

Casing thickness: 0.0127 m



Left Figure:

Axial-symmetric model

One current electrode (emitter)

Three voltage electrodes (collectors)

Objective:

Compute second diff. of potential for various depth angles and possibly with water invasion

Method of solution:

Fourier series expansion + change of coordinates + 2D goal-oriented hp-FEM

# NUMERICAL RESULTS: DC RESULTS

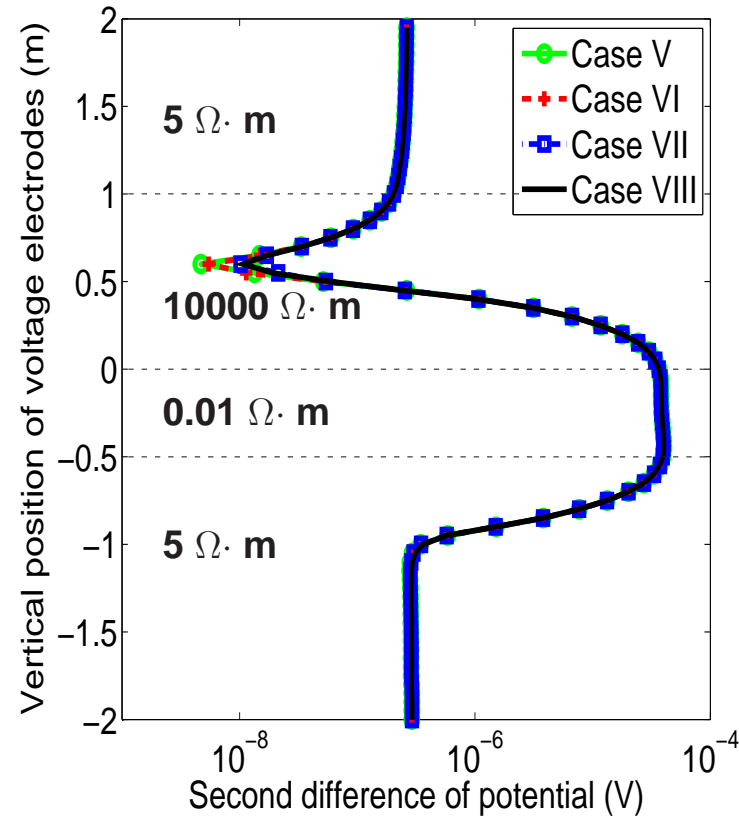
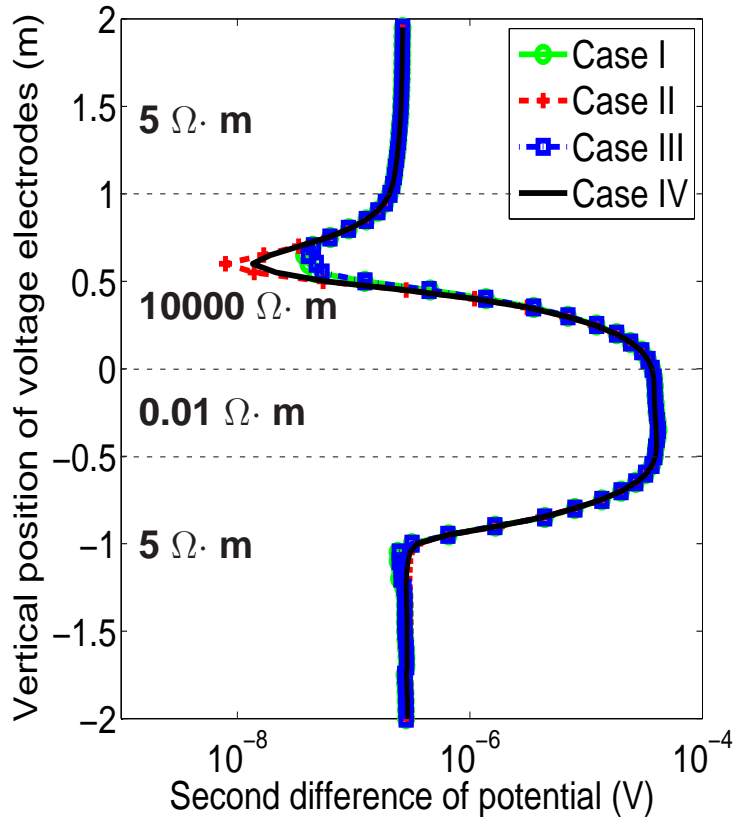
## Simulation of Through Casing Resistivity Measurements

Algorithm (Case) Number	I	II	III	IV	V	VI	VII	VIII
<b>1</b> Fourier mode used for adaptivity	X	X	X	X				
<b>5</b> Fourier modes used for adaptivity					X	X	X	X
Final <i>hp</i> -grid NOT <i>p</i> -enriched	X		X		X		X	
Final <i>hp</i> -grid globally <i>p</i> -enriched		X		X		X		X
<b>9</b> Fourier modes used for the final solution	X	X			X	X		
<b>15</b> Fourier modes used for the final solution			X	X			X	X

**Different algorithms provide different levels of accuracy**

# NUMERICAL RESULTS: DC RESULTS

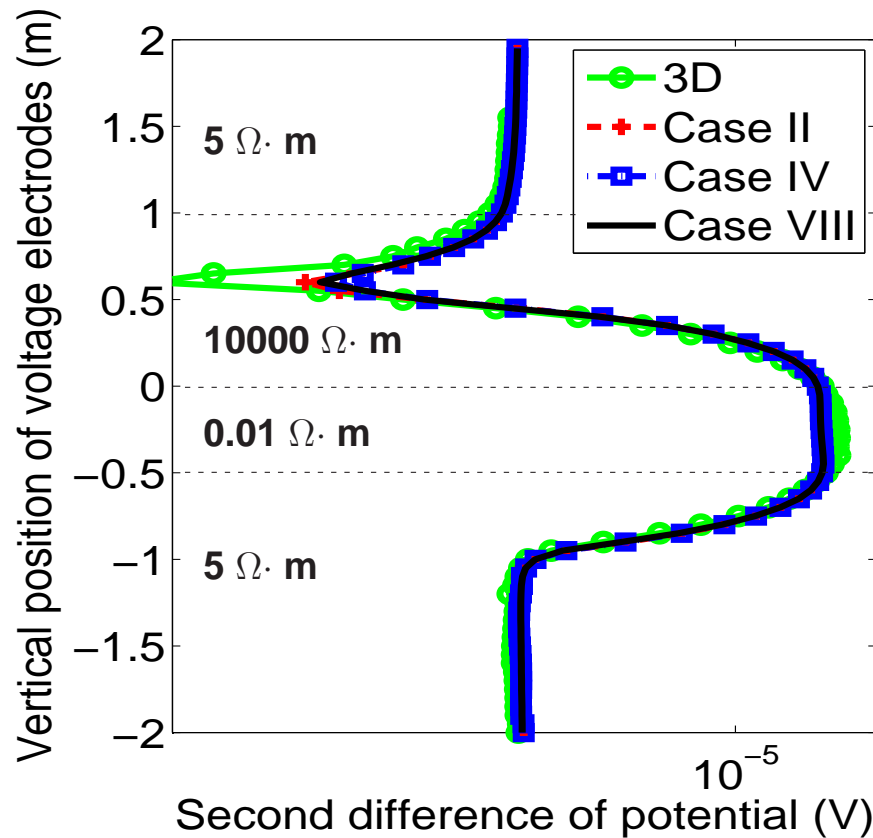
## Through Casing Resistivity Measurements (60-Degree Deviated Well)



Case Number	I	II	III	IV	V	VI	VII	VIII
Total Time (minutes)	21'	40'	39'	109'	244'	290'	286'	432'

# NUMERICAL RESULTS: DC RESULTS

## Through Casing Resistivity Measurements (60-Degree Deviated Well)



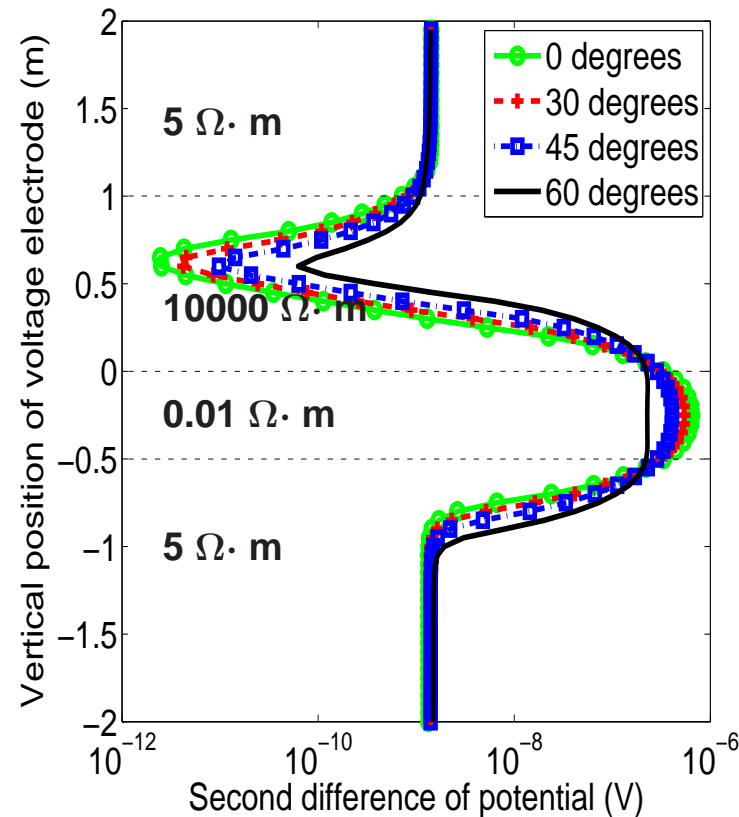
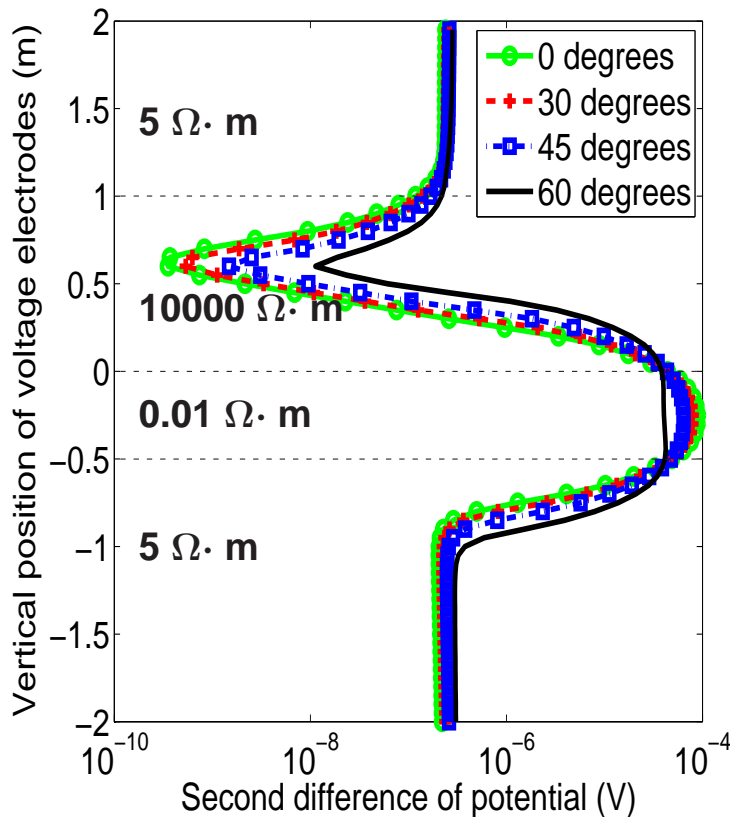
**Results with the new methodology seem more accurate than those obtained with the 3D software. In addition, with the new methodology we reduce the CPU time from several days to two hours.**

# NUMERICAL RESULTS: DC RESULTS

## Through Casing Resistivity Measurements (Casing Conductivity)

Casing Resistivity =  $10^{-5} \Omega \cdot m$

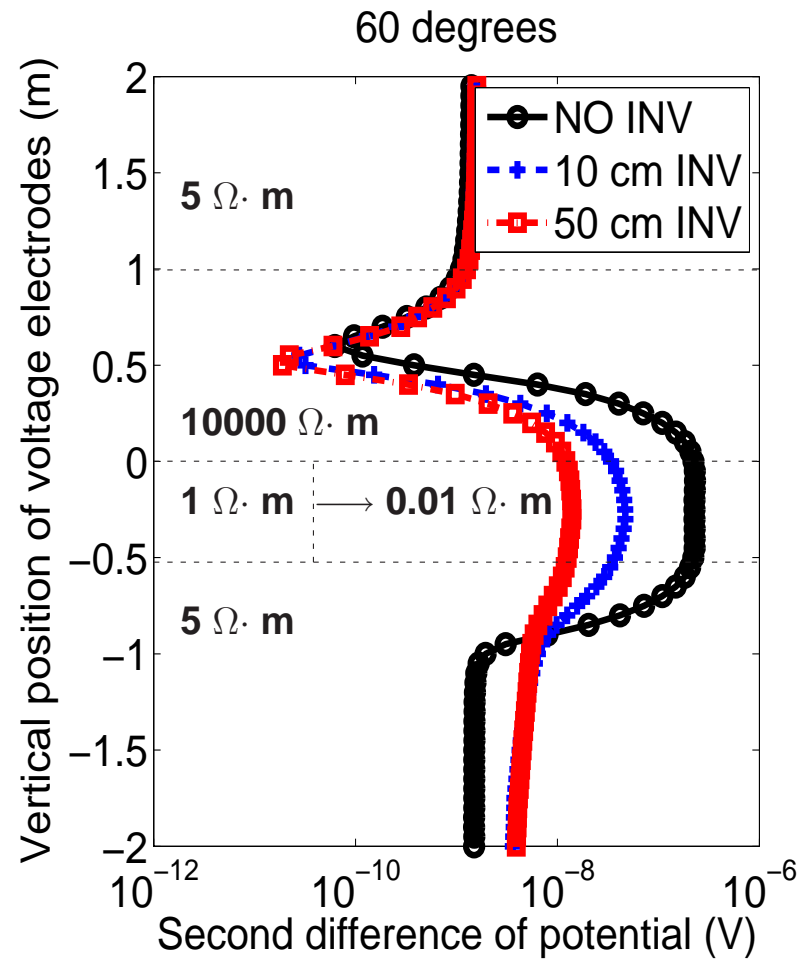
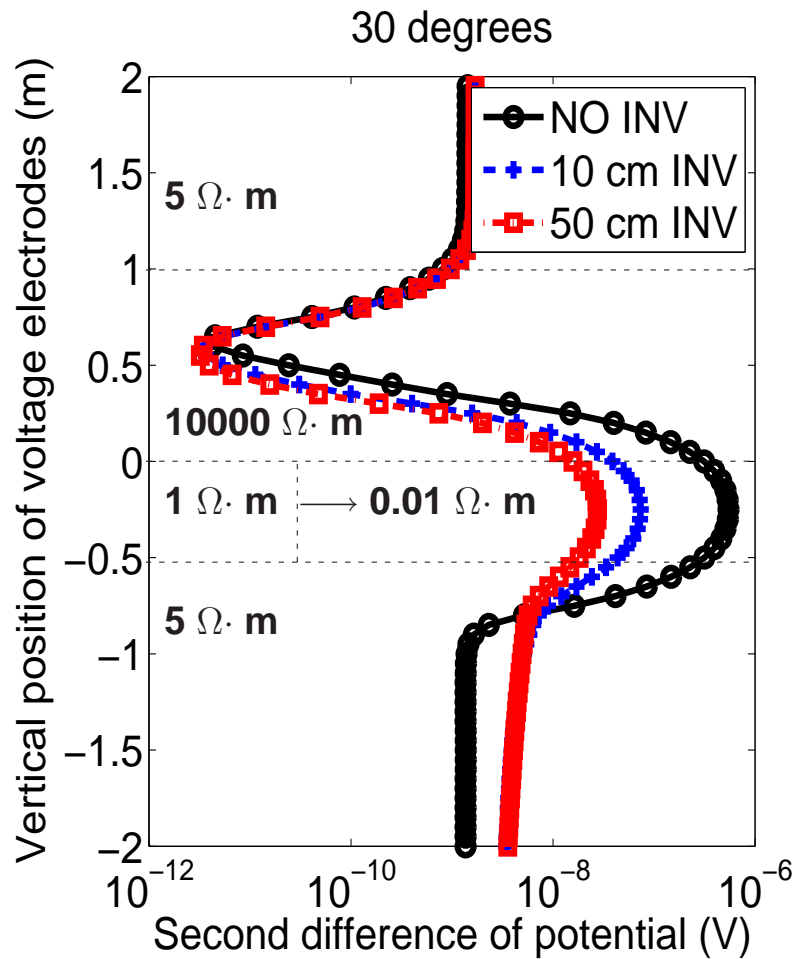
Casing Resistivity =  $2.3 \times 10^{-7} \Omega \cdot m$



**Qualitatively, results for various casing conductivities are similar even for deviated wells.**

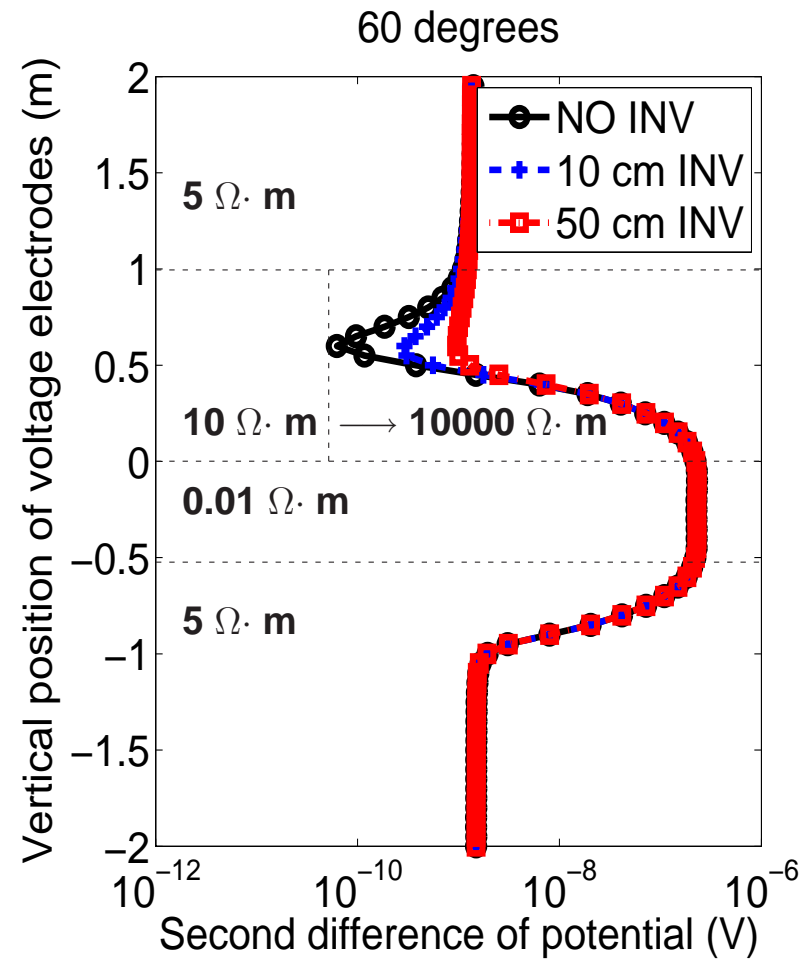
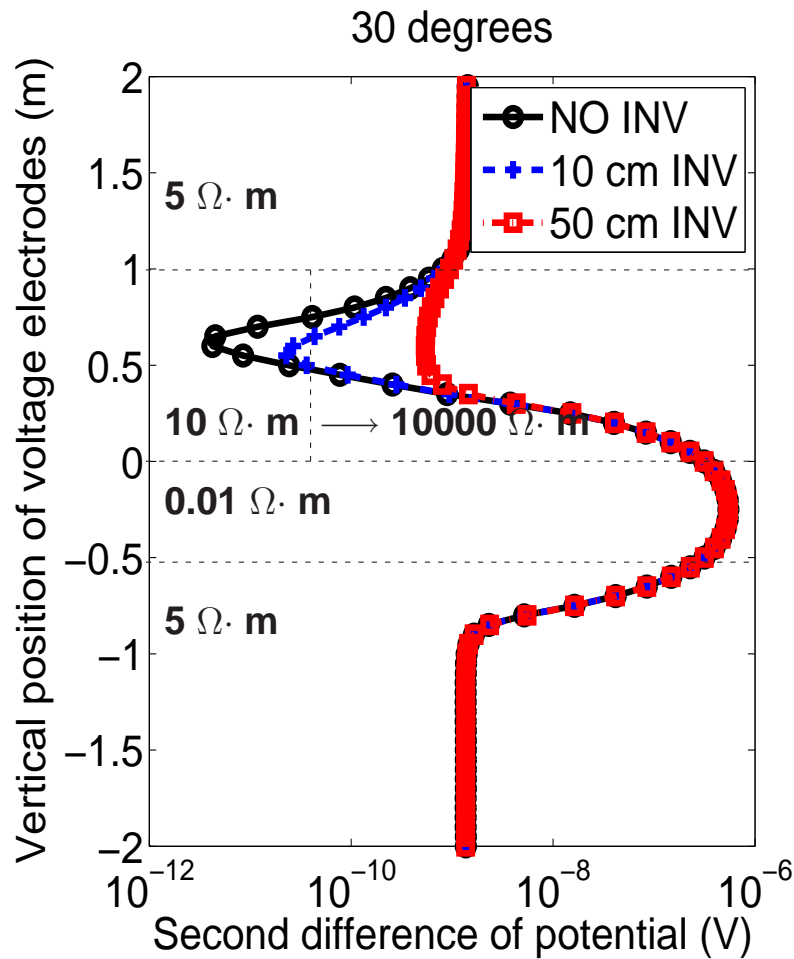
# NUMERICAL RESULTS: DC RESULTS

## Through Casing Resistivity Measurements (Invasion)



# NUMERICAL RESULTS: DC RESULTS

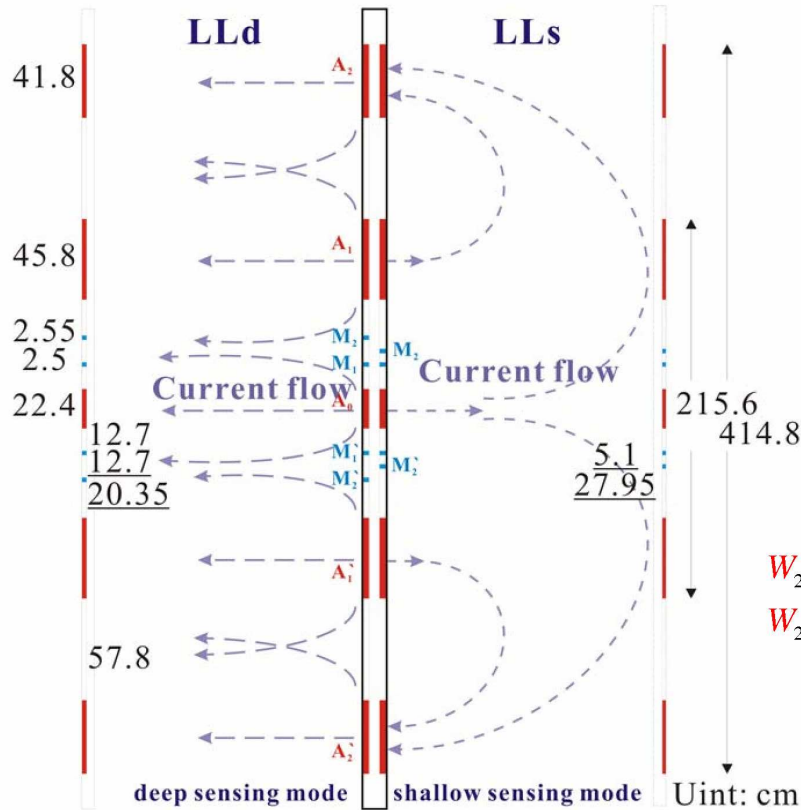
## Through Casing Resistivity Measurements (Invasion)



# NUMERICAL RESULTS: DC LATEROLOG

- Description of Tool

- Determination of Intensities ( $W_j$ ) of Bucking Currents



Focusing Conditions

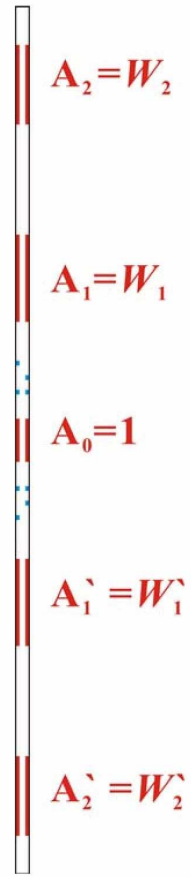
$$V(M_1) = V(M_2)$$

$$V(M_{1'}) = V(M_{2'})$$

Relationships between  $W_j$

$$W_2 = (W_1 + c), \quad W_{2'} = (W_{1'} + c) \text{ for LLd}$$

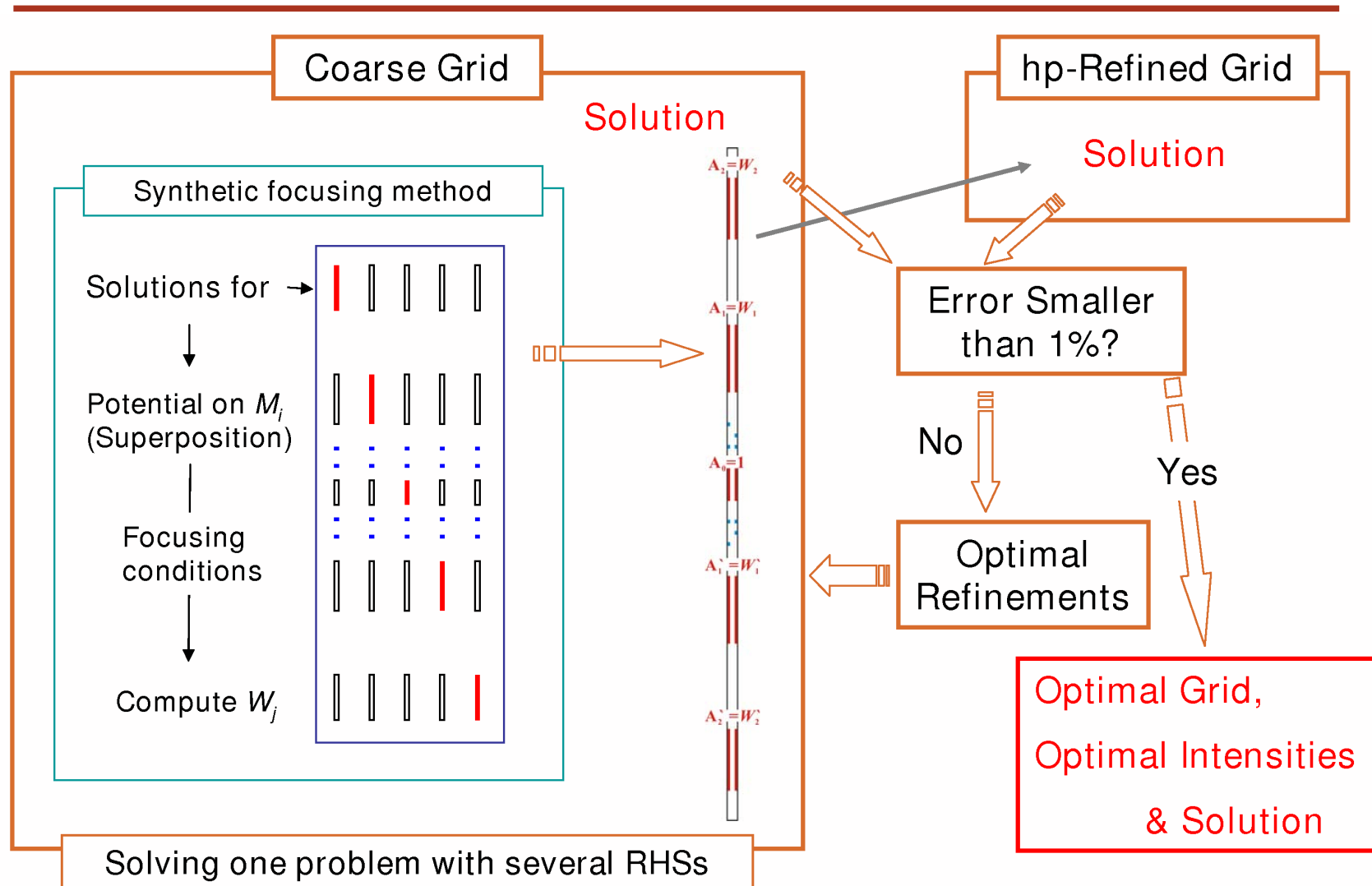
$$W_2 = -(W_1 + c), \quad W_{2'} = -(W_{1'} + c) \text{ for LLs}$$



DUAL LATEROLOG - Halliburton Energy Services



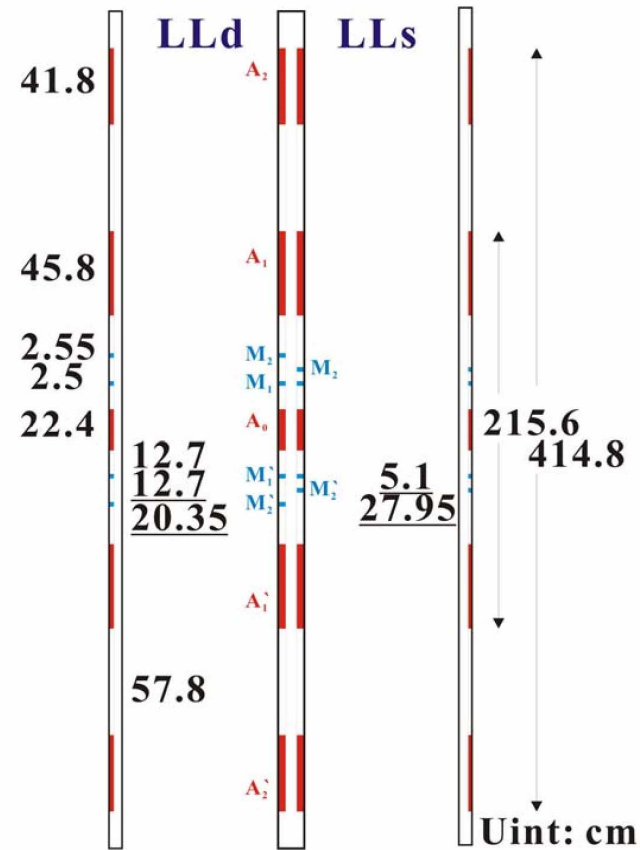
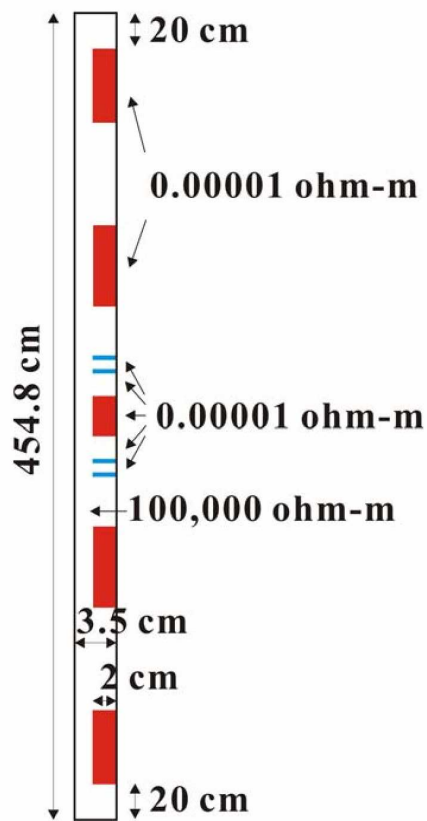
# NUMERICAL RESULTS: DC LATEROLOG



# NUMERICAL RESULTS: DC LATEROLOG

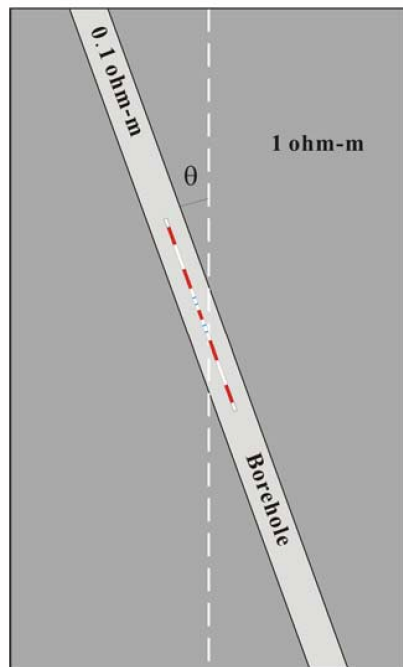
Model

Using the Tool Configuration of Halliburton Energy Services' DLL

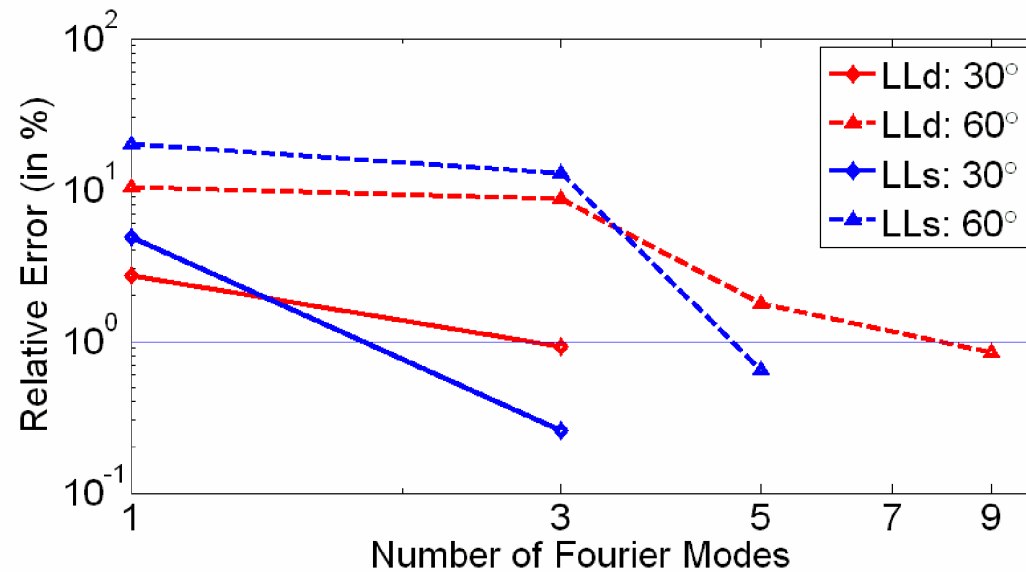


# NUMERICAL RESULTS: DC LATEROLOG

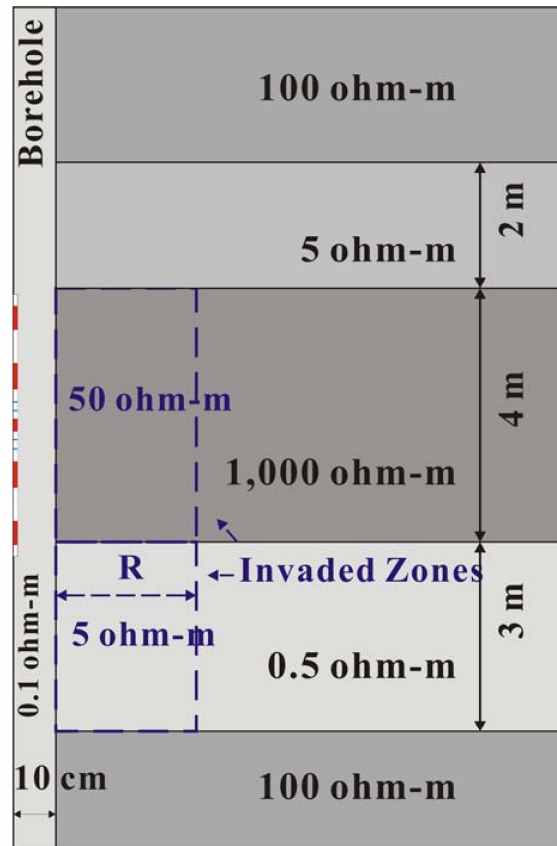
$\theta = 0, 30$  and  $60$  degrees



Relative errors of laterolog instruments in a homogeneous formation



# NUMERICAL RESULTS: DC LATEROLOG



Five layers: 100, 5, 1000, 0.5 and 100 ohm-m from top to bottom

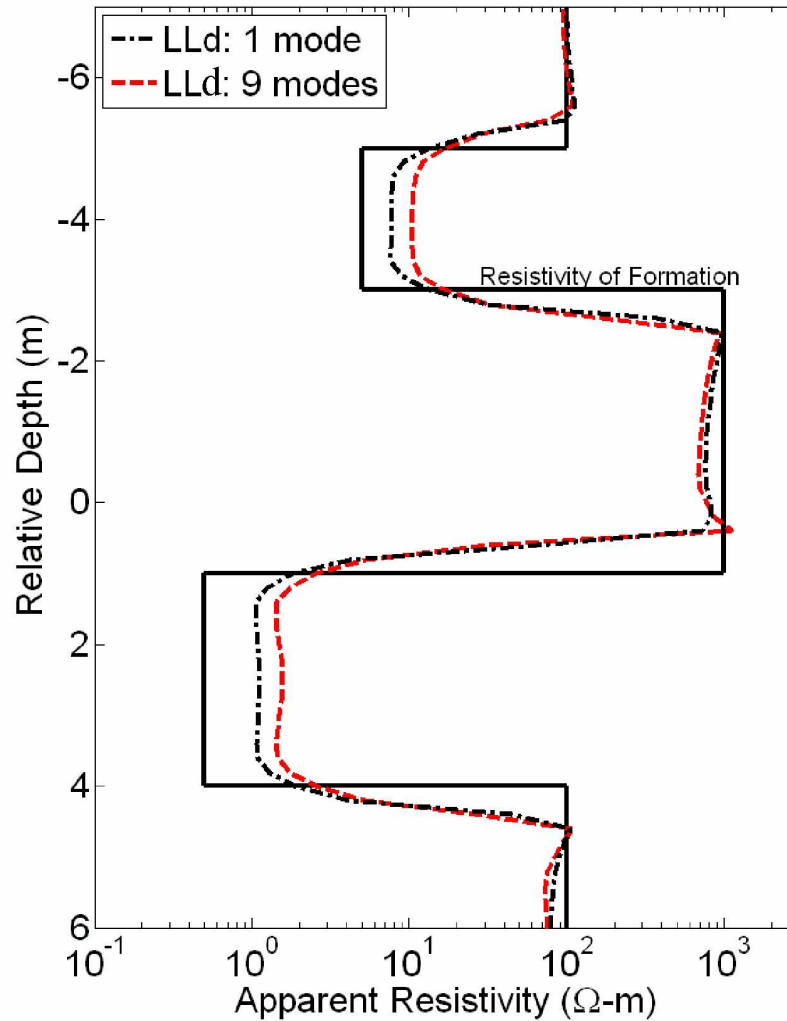
Borehole: 0.1 m in radius  
0.1 ohm-m in resistivity

Invasion

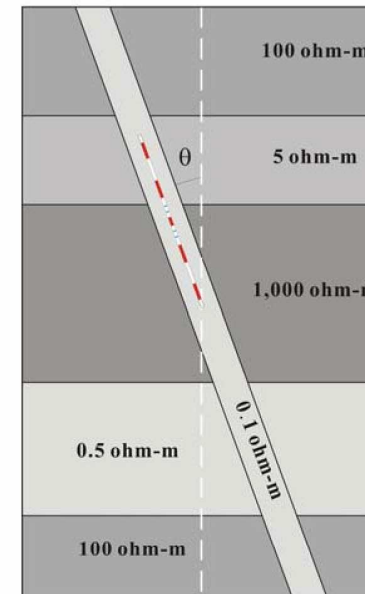
Anisotropy

# NUMERICAL RESULTS: DC LATEROLOG

Comparison of Solutions by 1 and 9 Fourier Modes

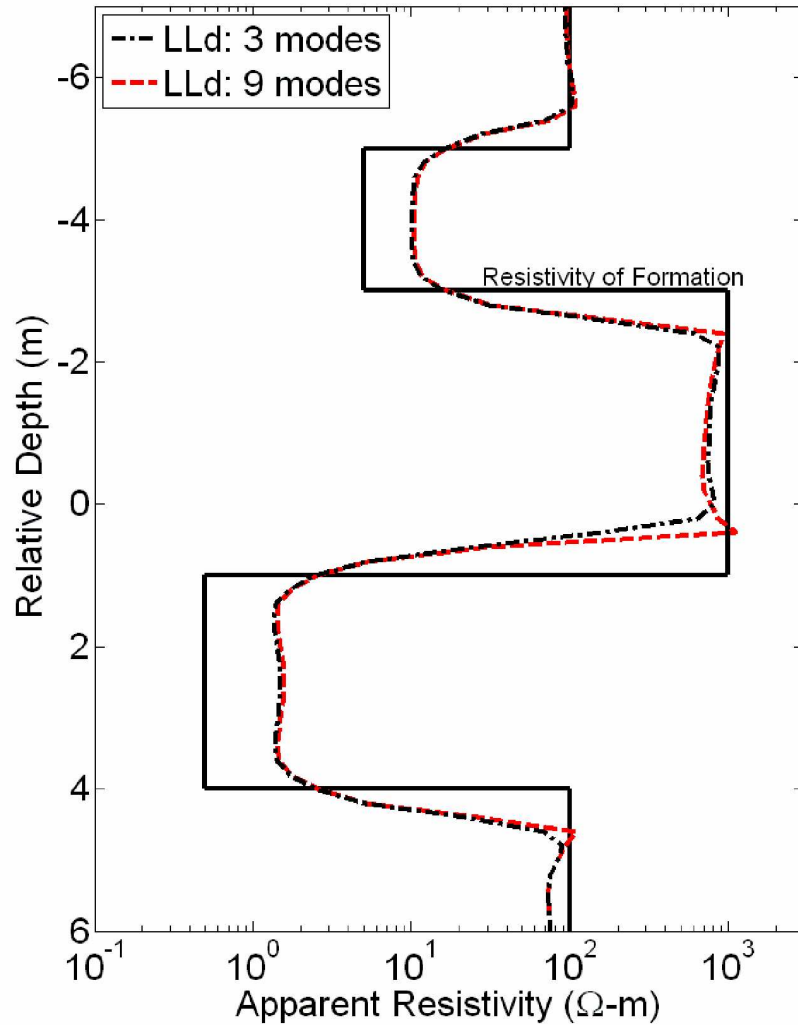


Dip angle: 45 degrees

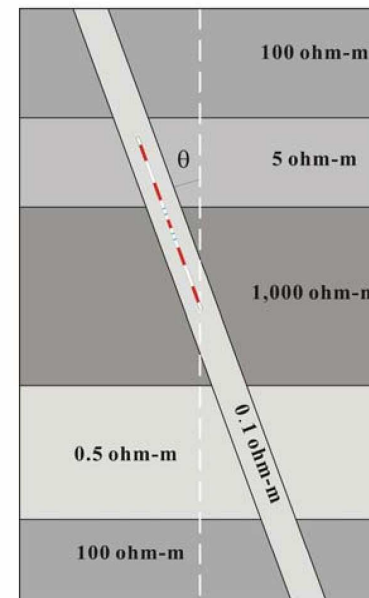


# NUMERICAL RESULTS: DC LATEROLOG

Comparison of Solutions by 3 and 9 Fourier Modes

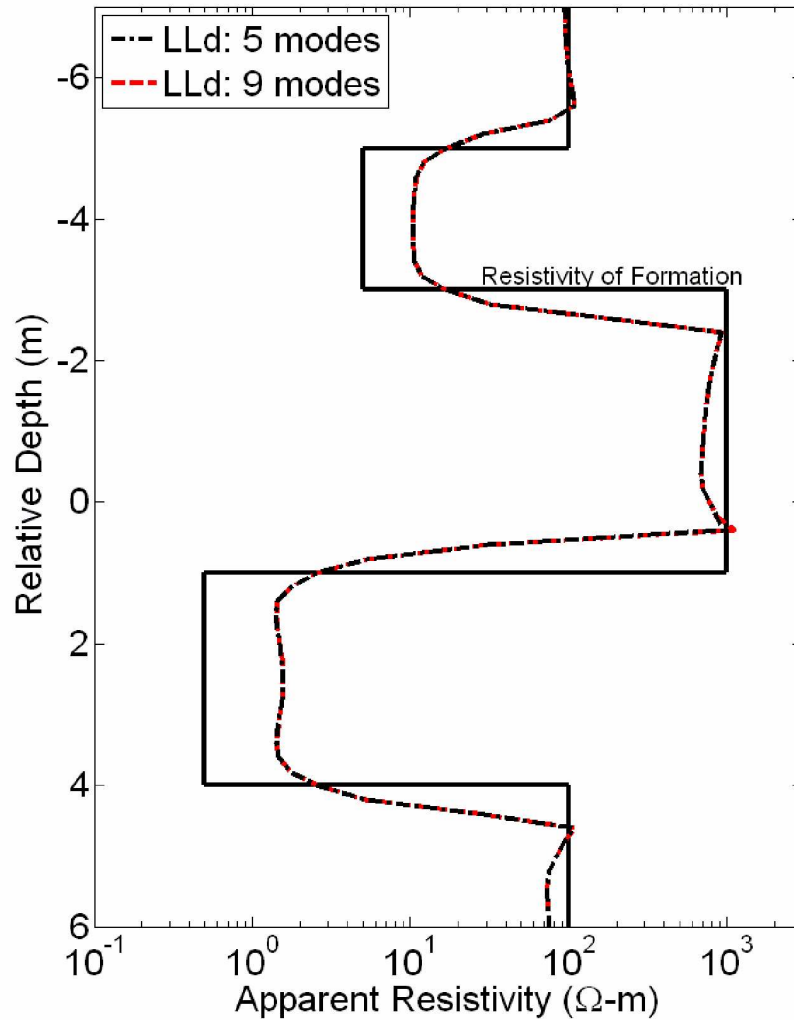


Dip angle: 45 degrees

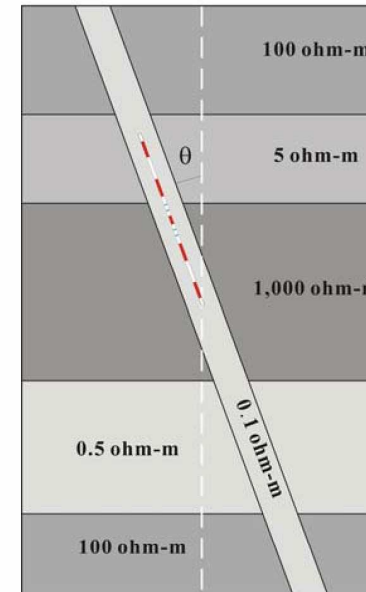


# NUMERICAL RESULTS: DC LATEROLOG

Comparison of Solutions by 5 and 9 Fourier Modes

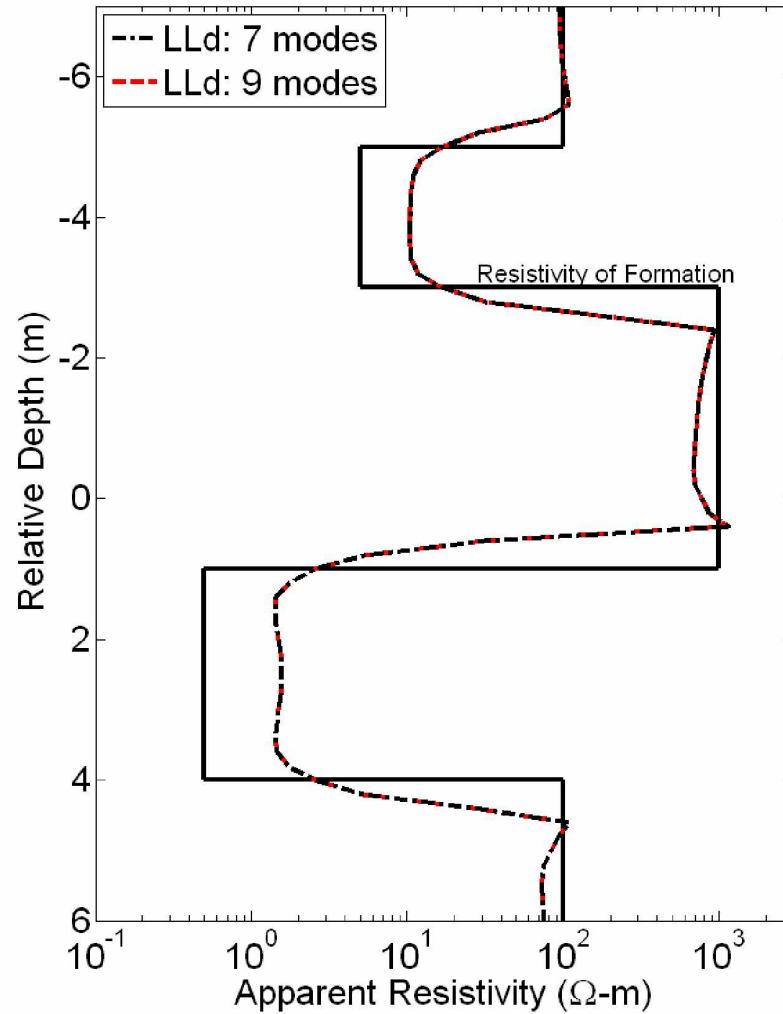


Dip angle: 45 degrees

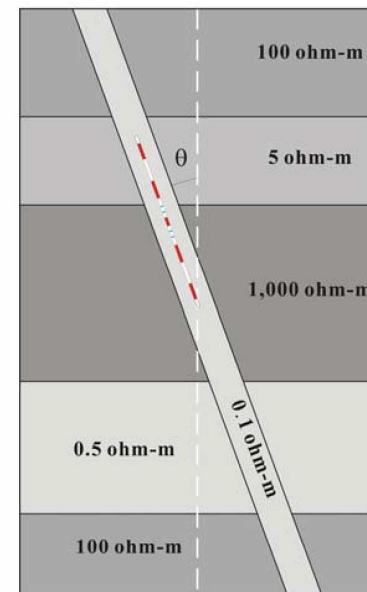


# NUMERICAL RESULTS: DC LATEROLOG

Comparison of Solutions by 7 and 9 Fourier Modes

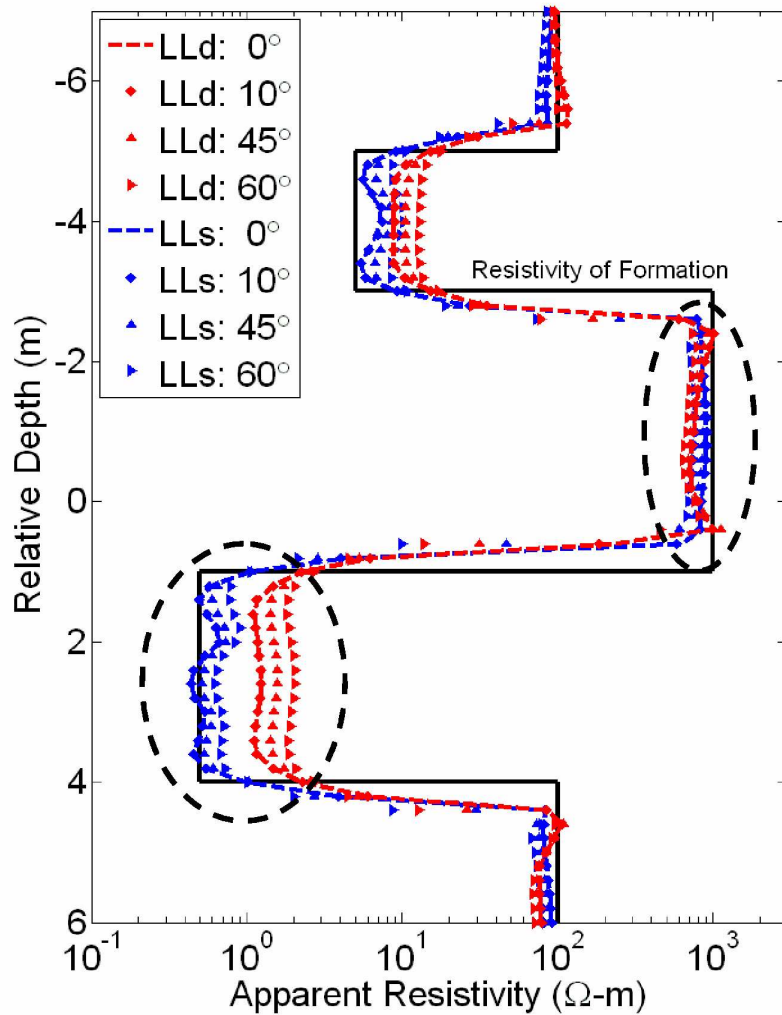


Dip angle: 45 degrees

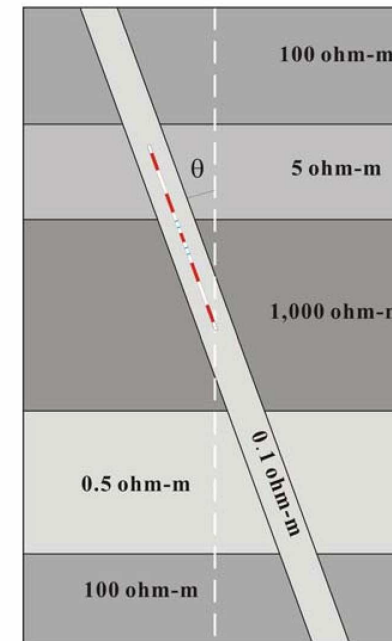




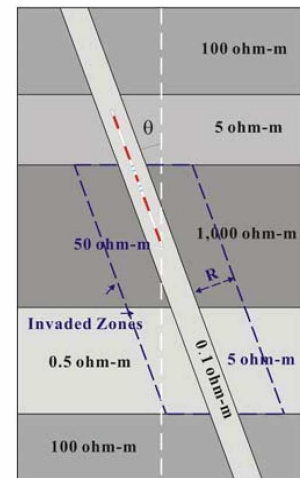
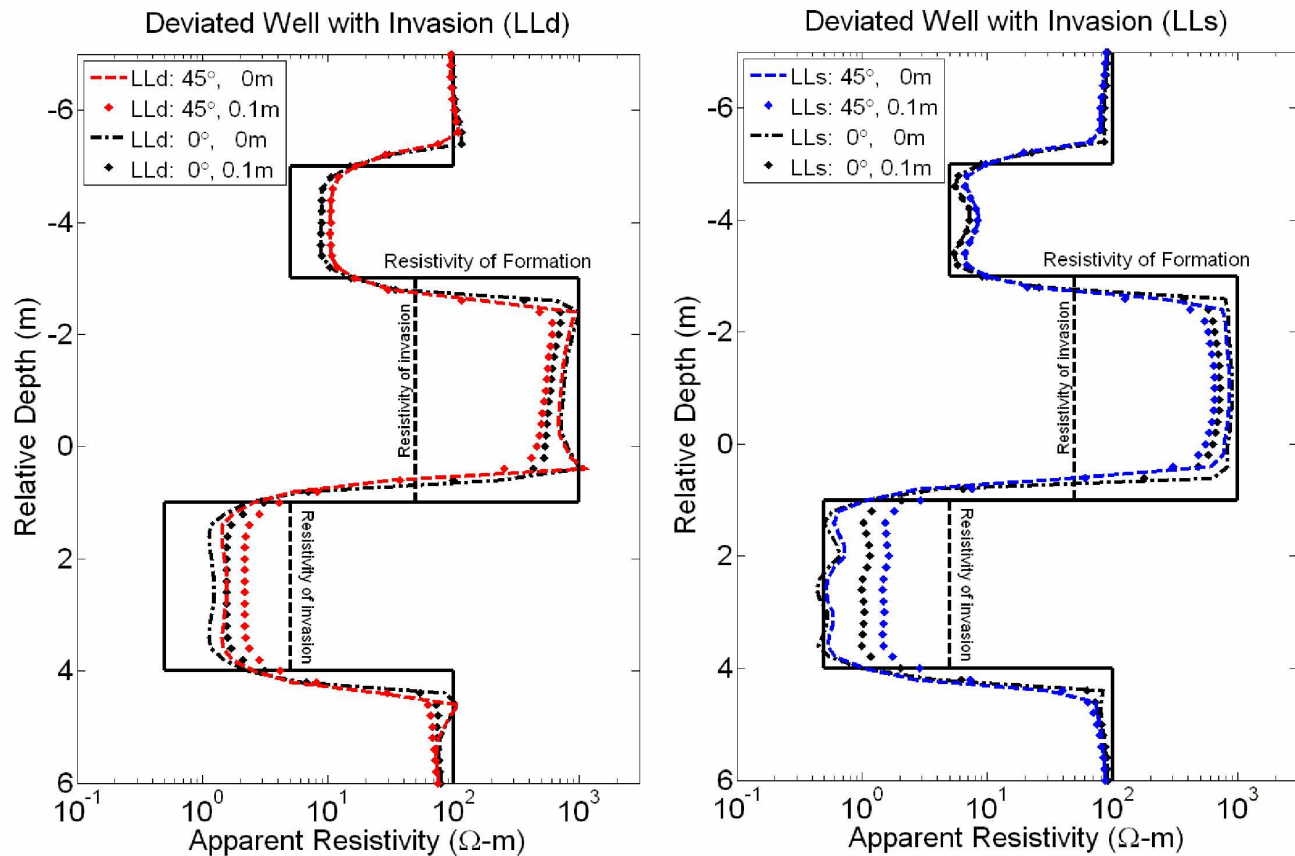
# NUMERICAL RESULTS: DC LATEROLOG



Effects of dip angle: Conductive layer  $\uparrow$

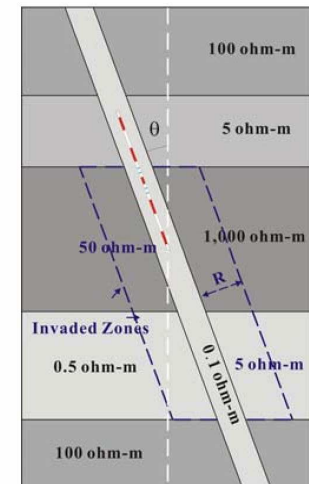
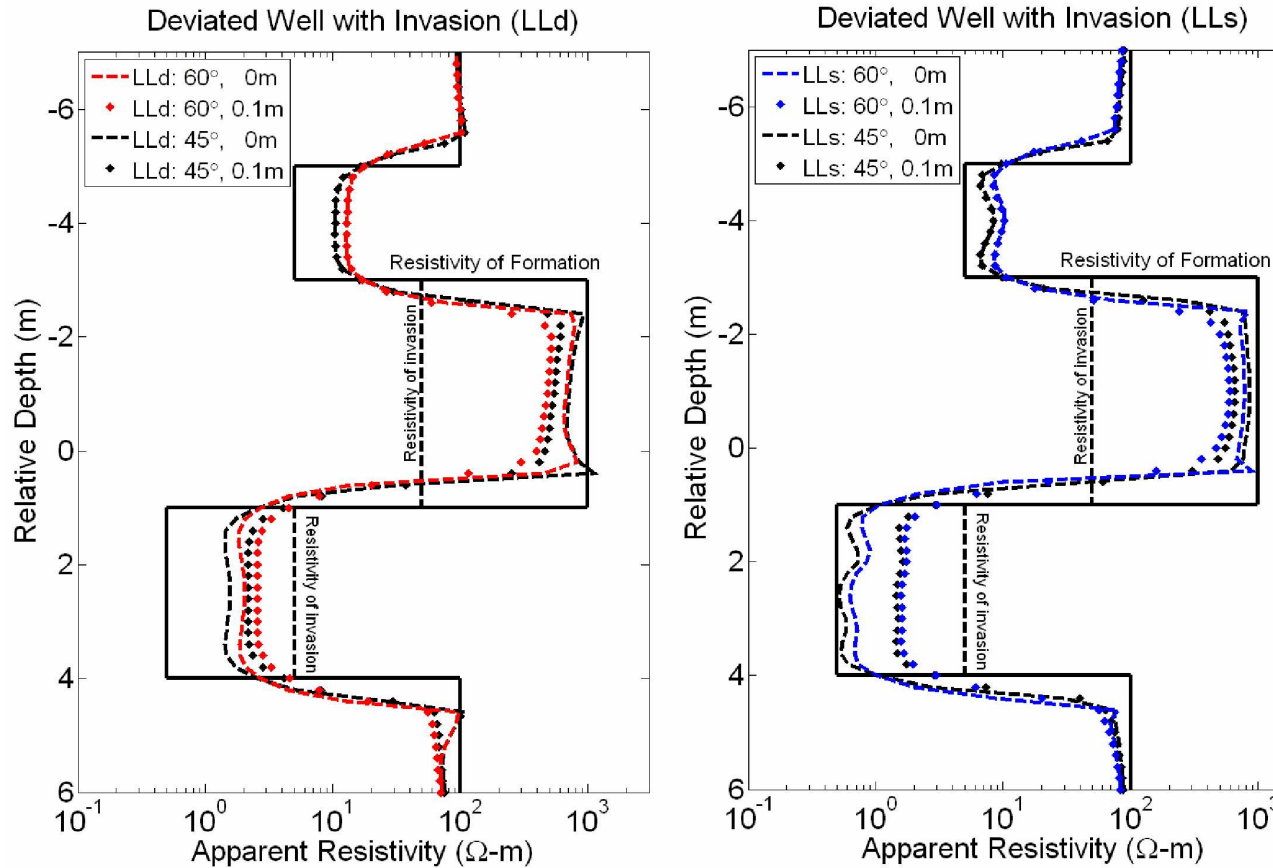


# NUMERICAL RESULTS: DC LATEROLOG



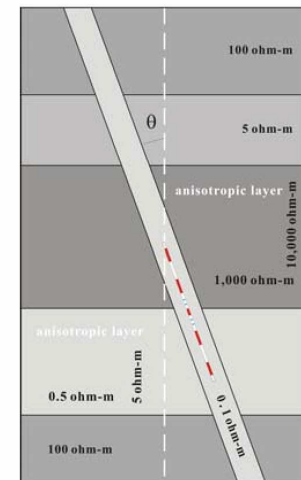
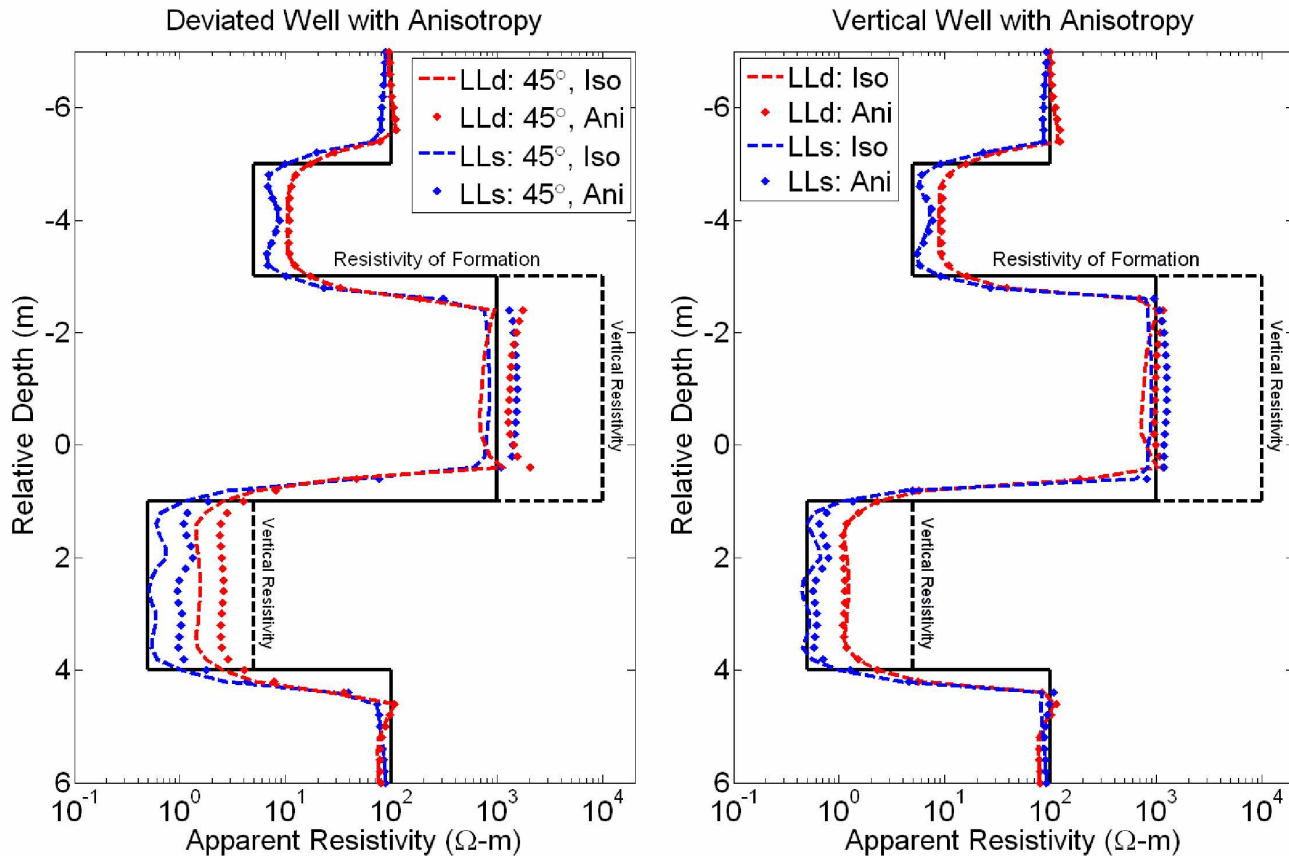
Effects of invasion to LLs: larger in a 45-degree deviated well than in a vertical well in conductive layer

# NUMERICAL RESULTS: DC LATEROLOG



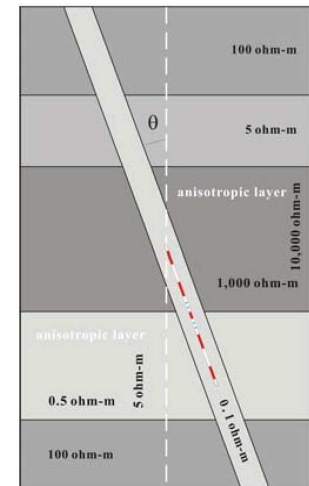
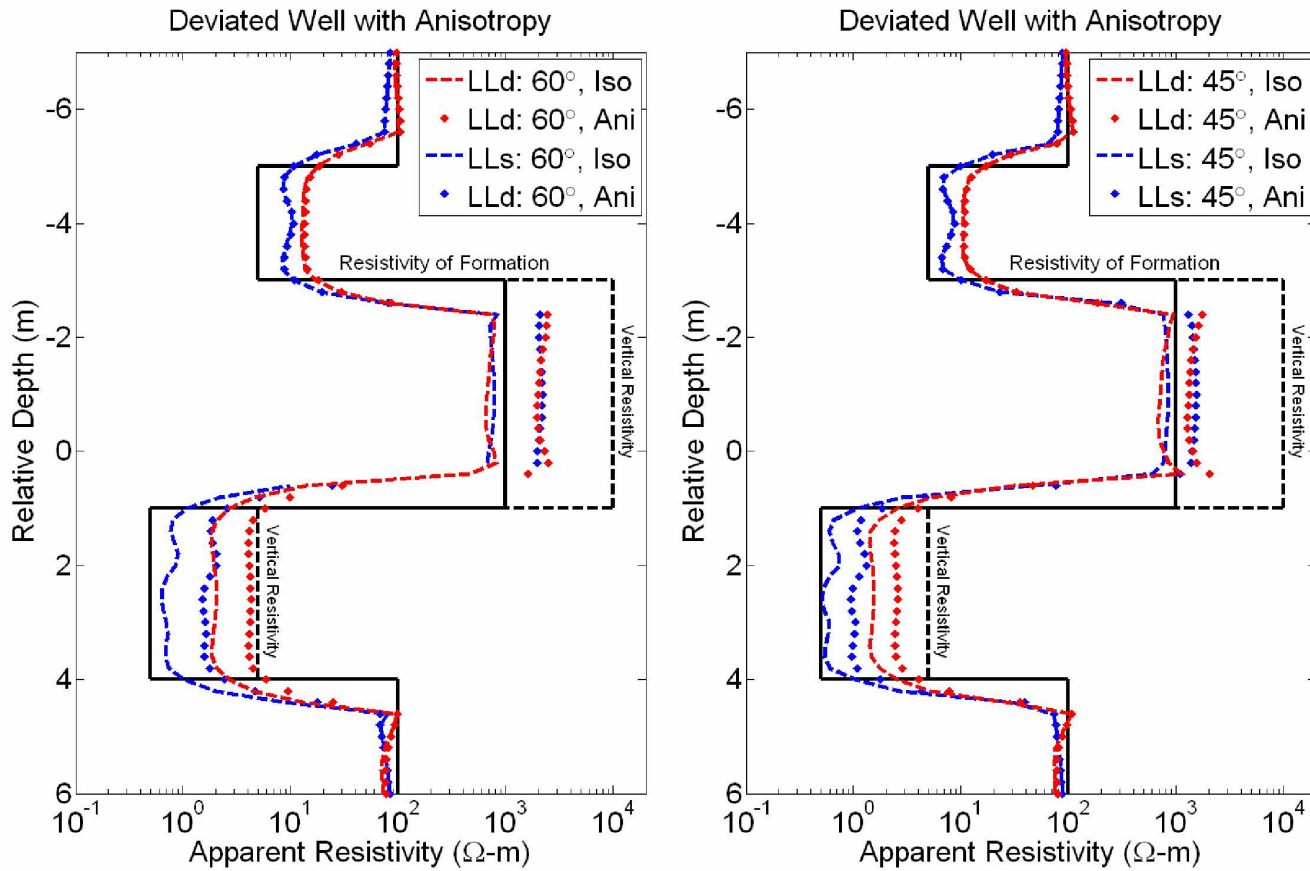
Effects of invasion to LLs: slightly smaller in a 60-degree deviated well than in a 45-degree deviated well in conductive layer

# NUMERICAL RESULTS: DC LATEROLOG



Effects of anisotropy: 45-degree deviated well ↑

# NUMERICAL RESULTS: DC LATEROLOG

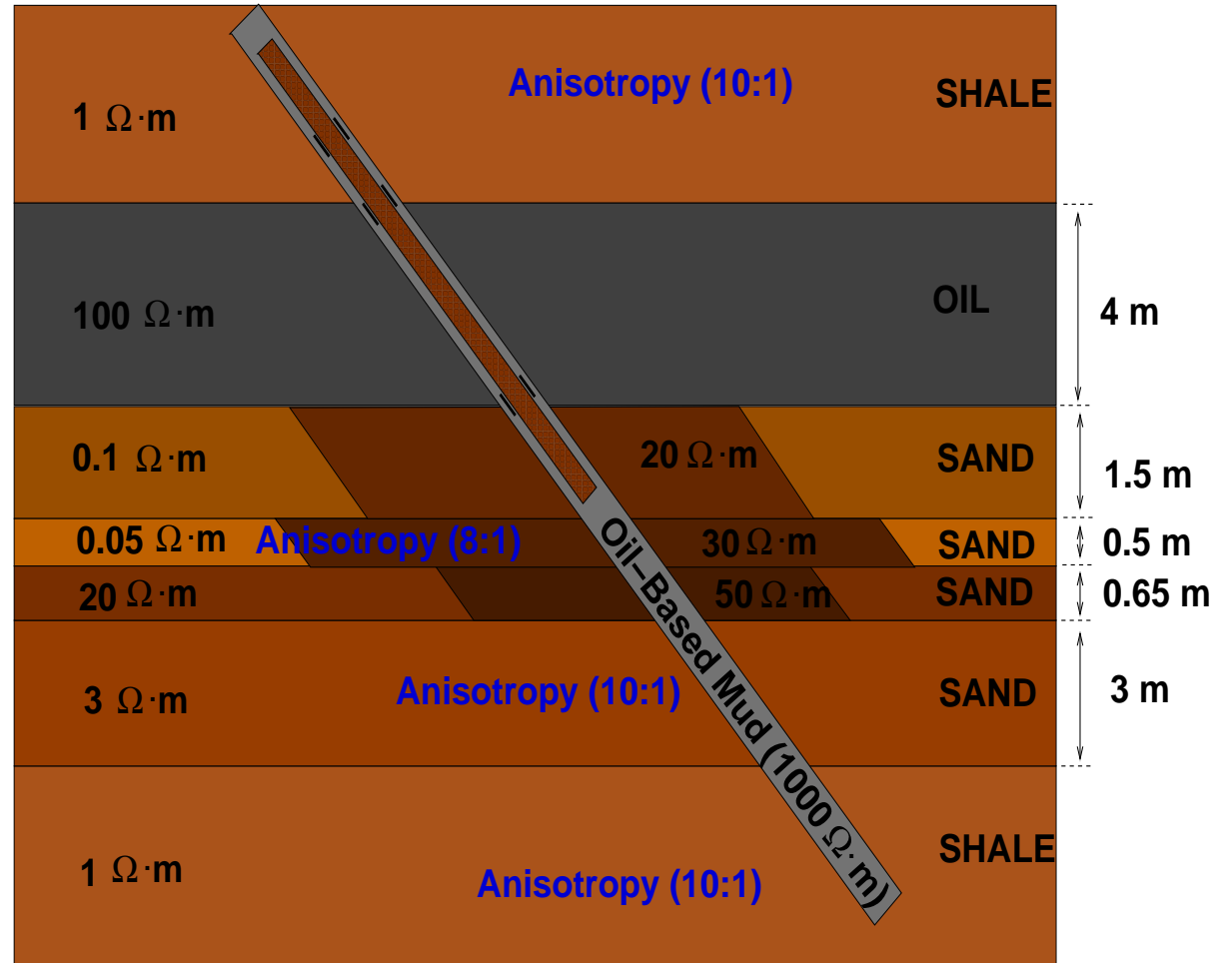
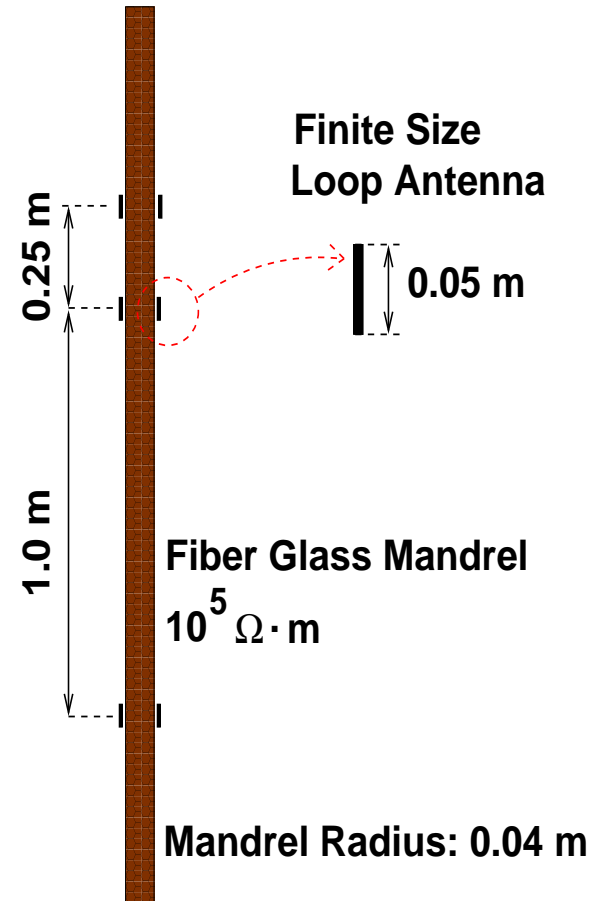


Effects of anisotropy: 60-degree deviated well ↑

# NUMERICAL RESULTS: AC RESULTS

## Model Problem

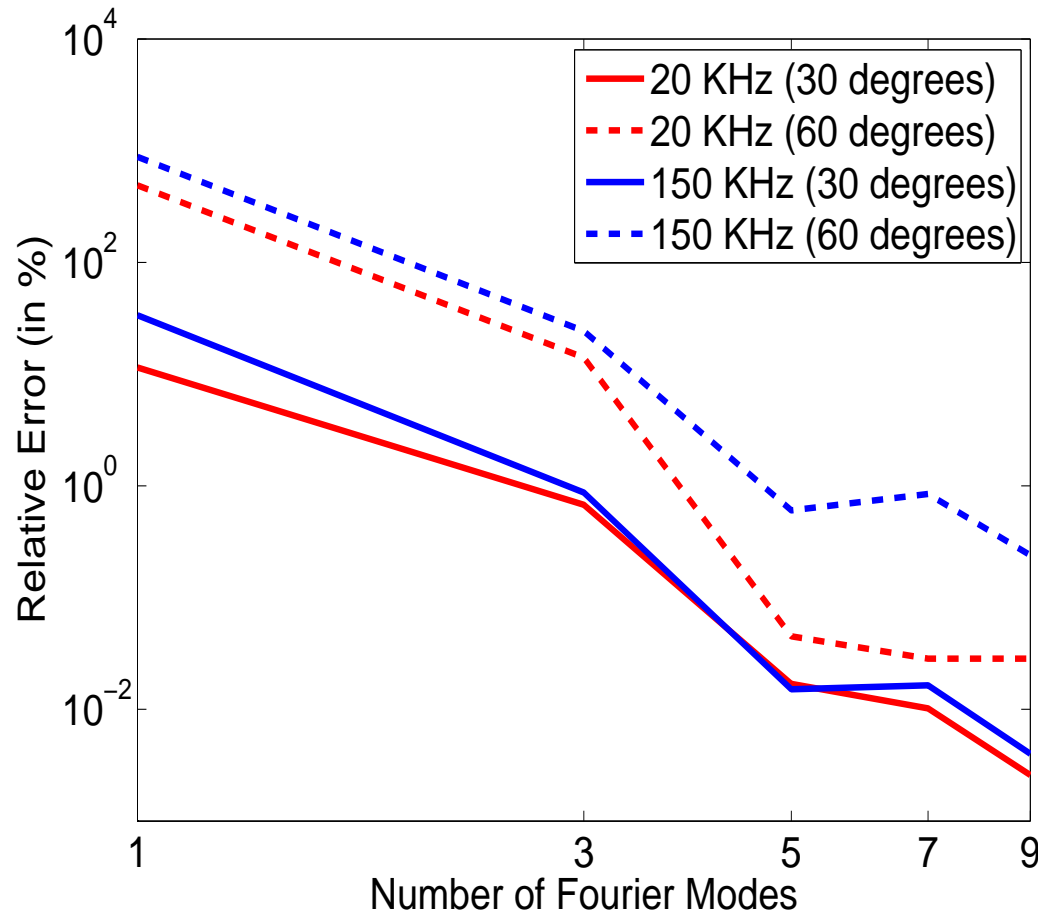
150 kHz (Wireline)



# NUMERICAL RESULTS: AC RESULTS

## Verification

### Logging Instrument in a Homogeneous Formation

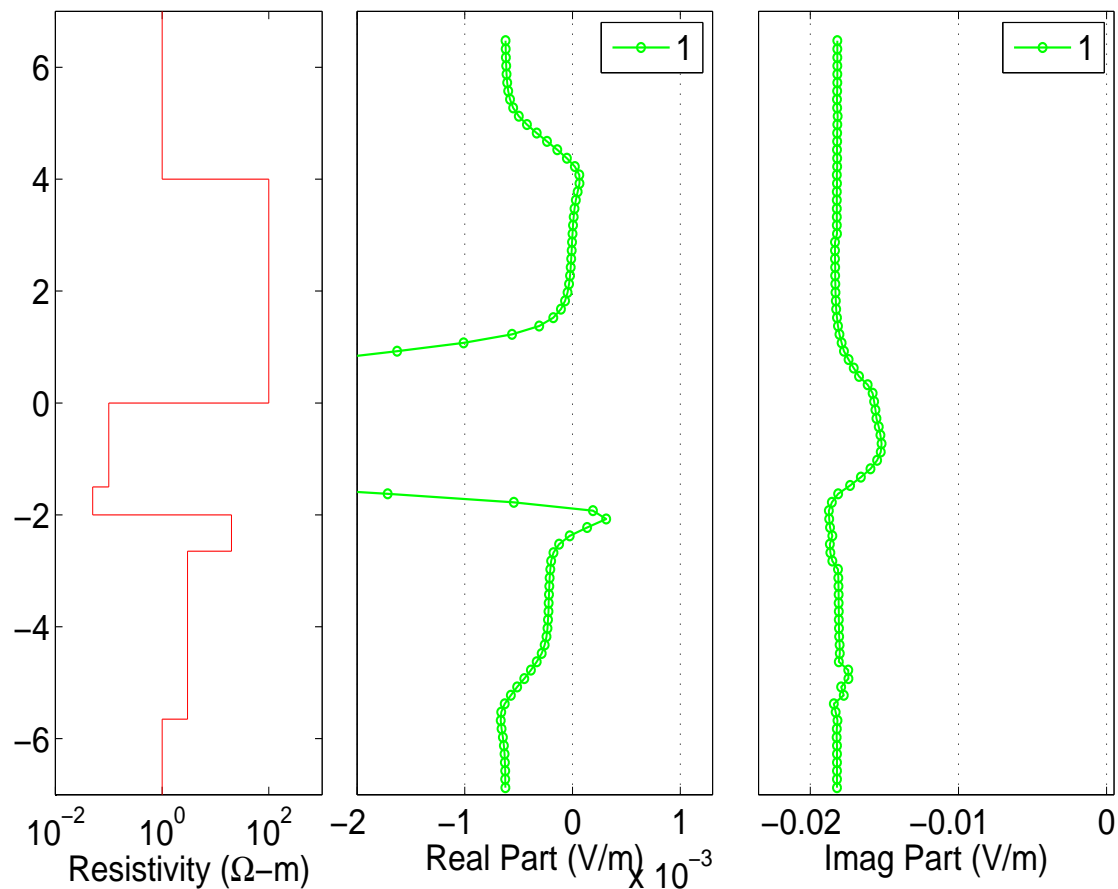


# NUMERICAL RESULTS: AC RESULTS

## Verification

### Logging Instrument in a Homogeneous Formation

Wireline, 150 Khz



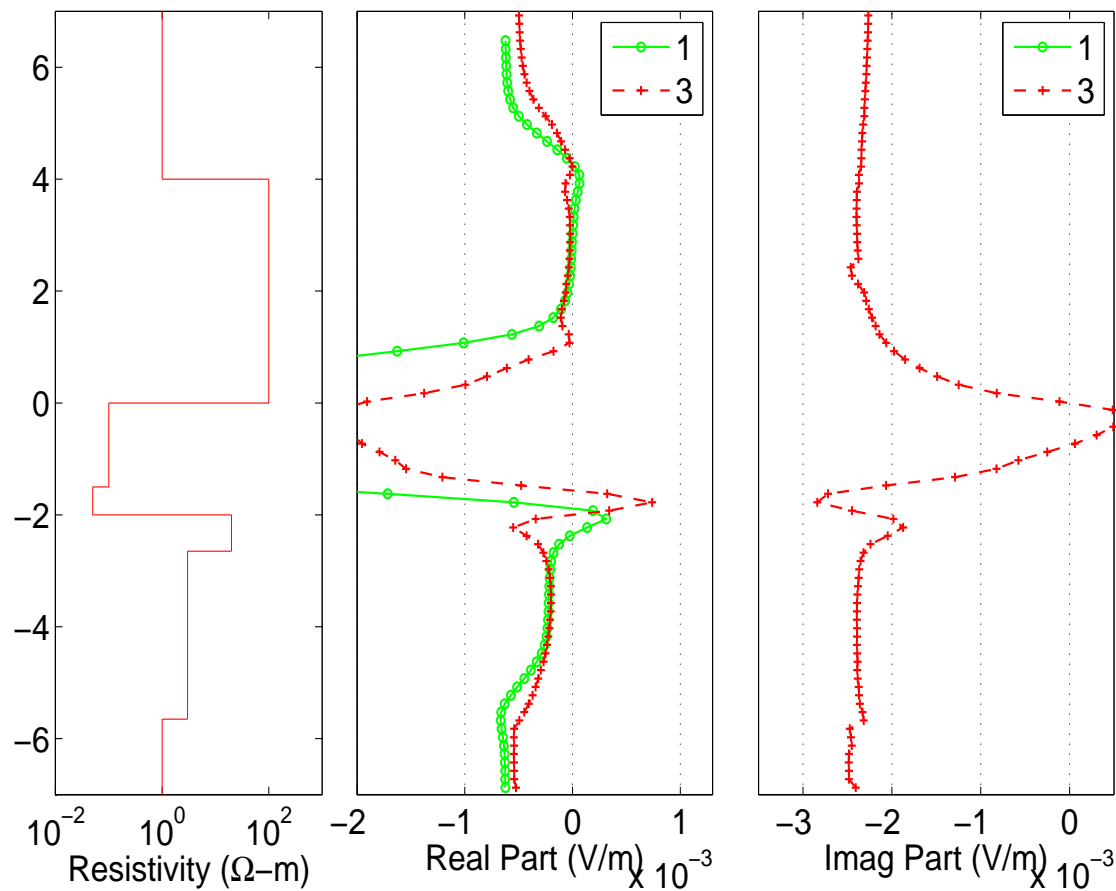


# NUMERICAL RESULTS: AC RESULTS

## Verification

### Logging Instrument in a Homogeneous Formation

Wireline, 150 Khz

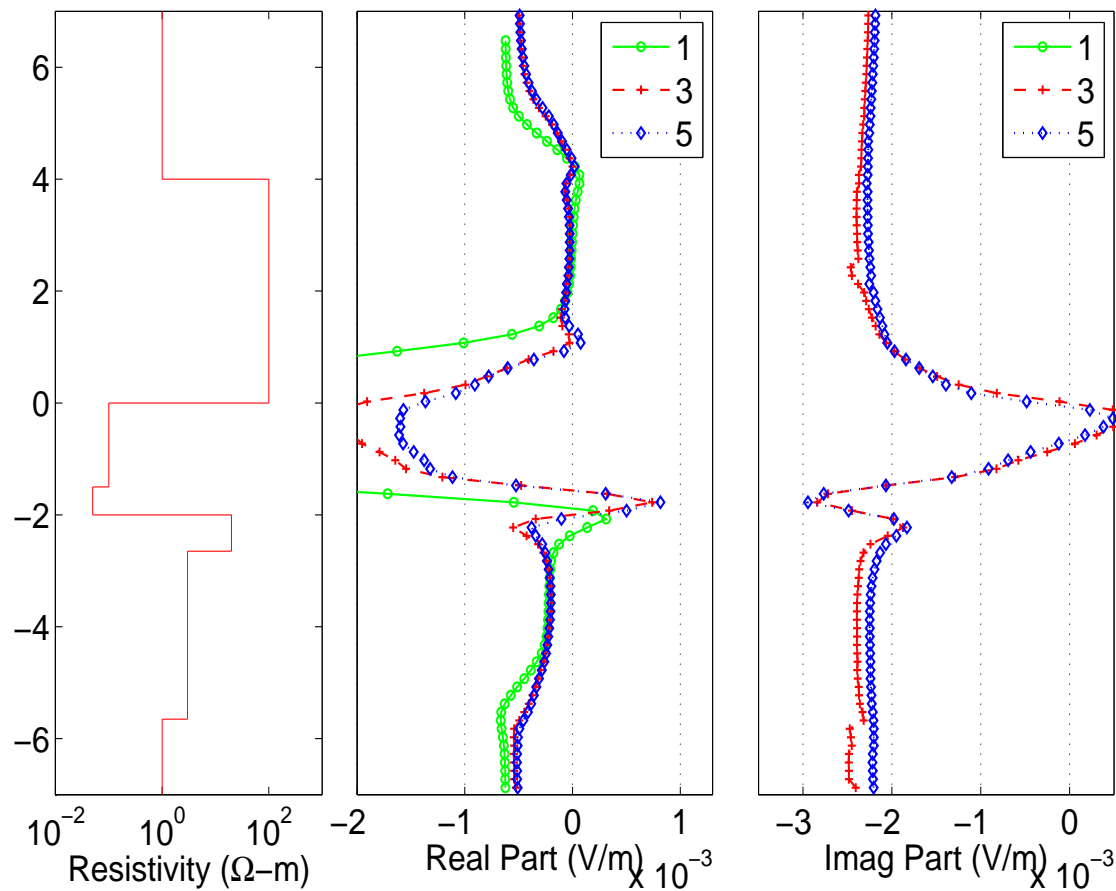


# NUMERICAL RESULTS: AC RESULTS

## Verification

### Logging Instrument in a Homogeneous Formation

Wireline, 150 Khz

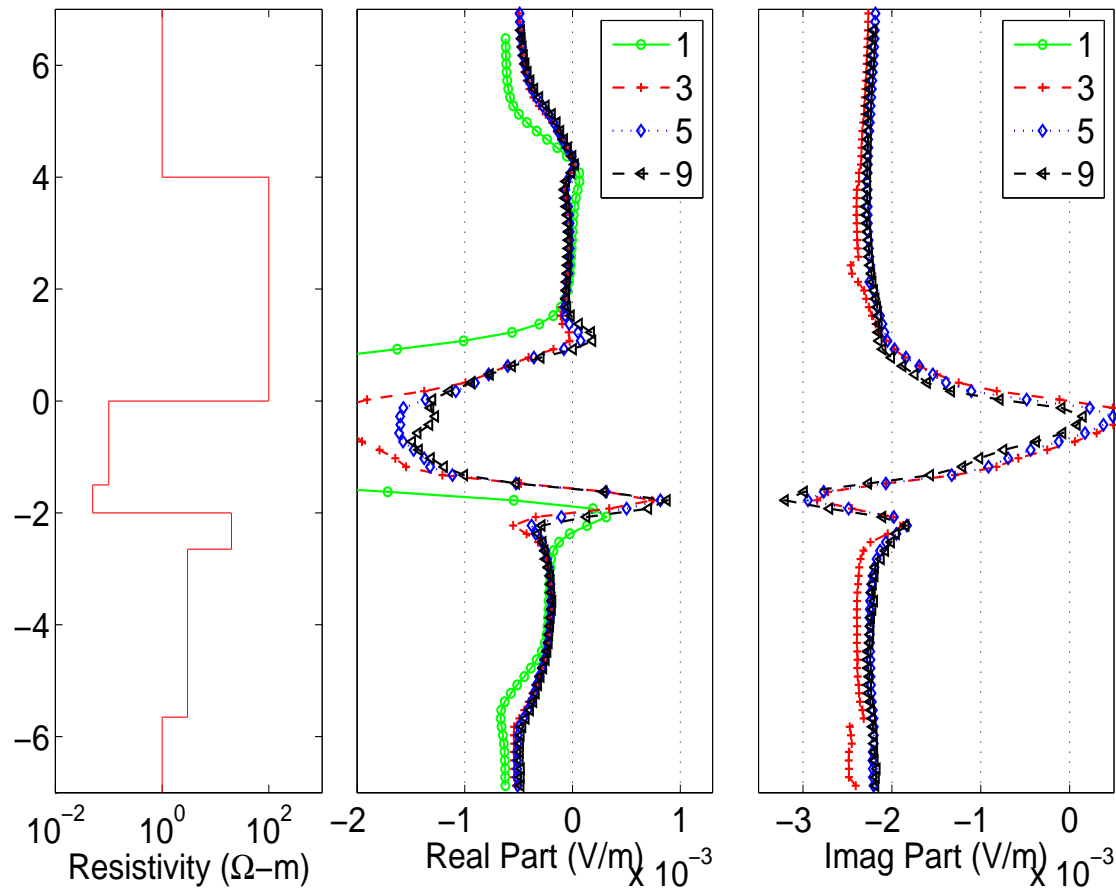


# NUMERICAL RESULTS: AC RESULTS

## Verification

### Logging Instrument in a Homogeneous Formation

Wireline, 150 Khz

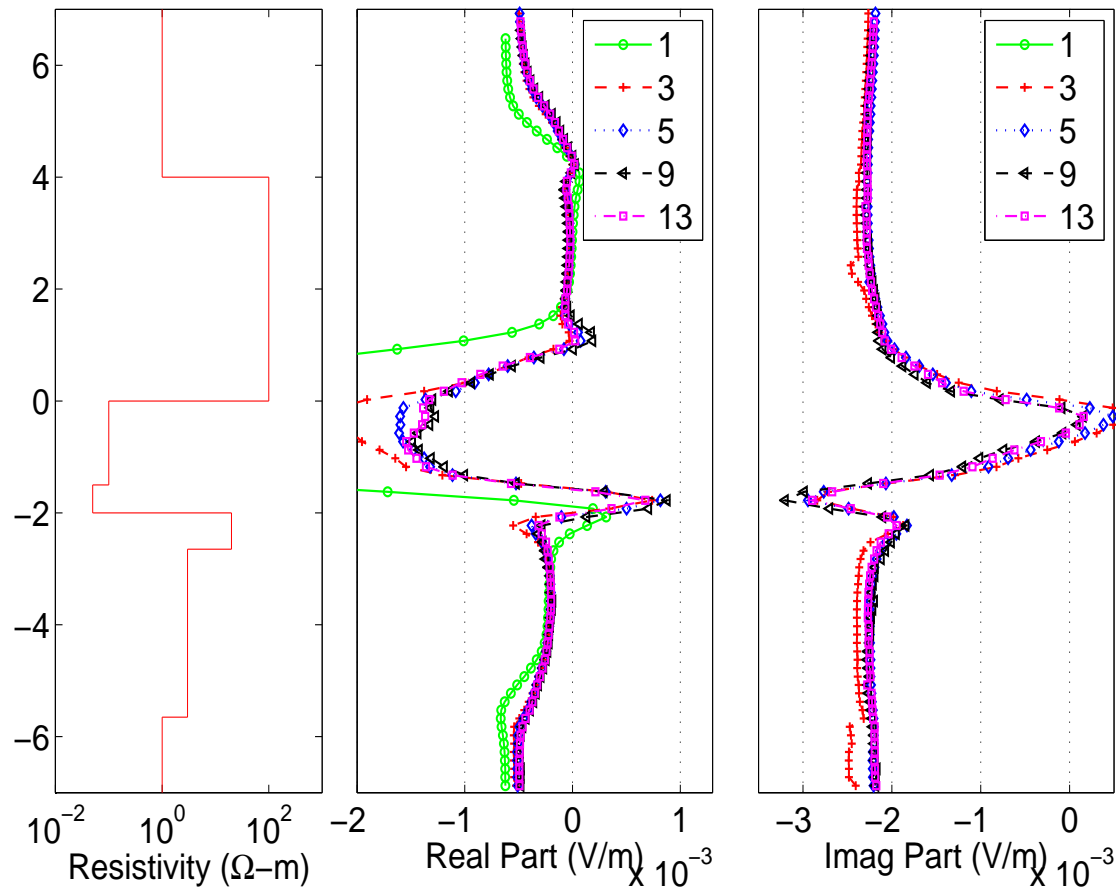


# NUMERICAL RESULTS: AC RESULTS

## Verification

### Logging Instrument in a Homogeneous Formation

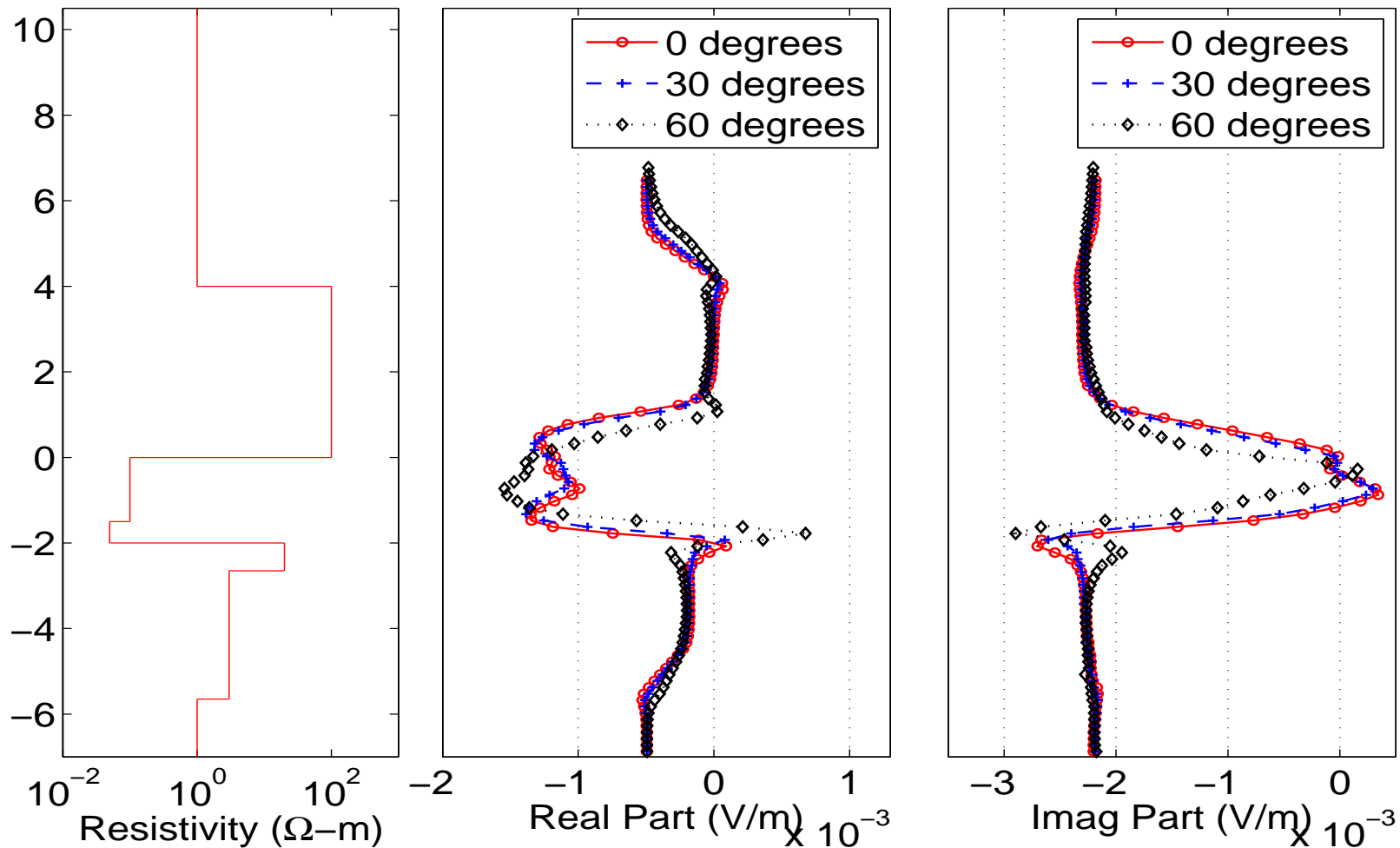
Wireline, 150 Khz



# NUMERICAL RESULTS: AC RESULTS

## Dip Angle

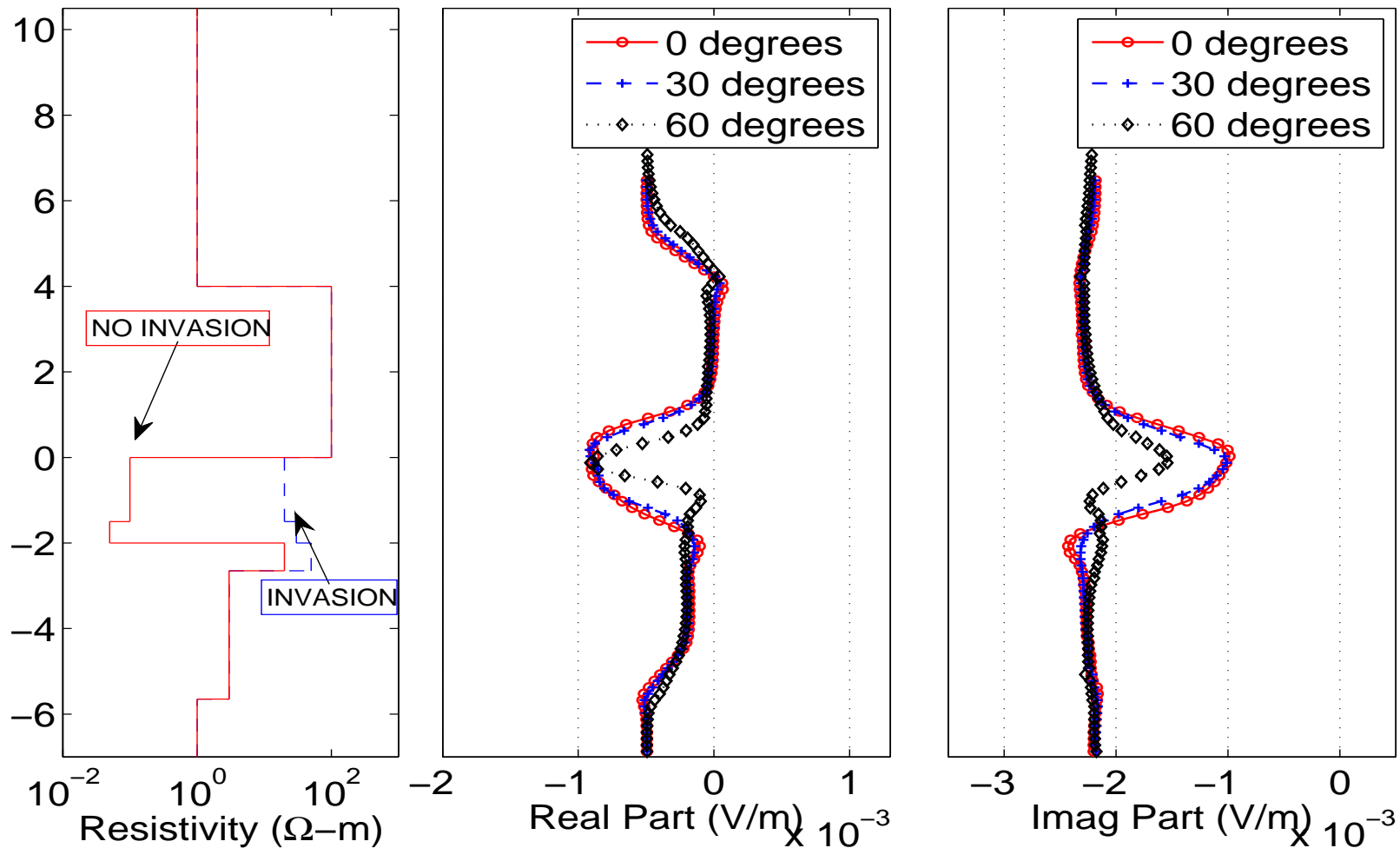
Wireline, 150 Khz



# NUMERICAL RESULTS: AC RESULTS

## Dip Angle + Invasion

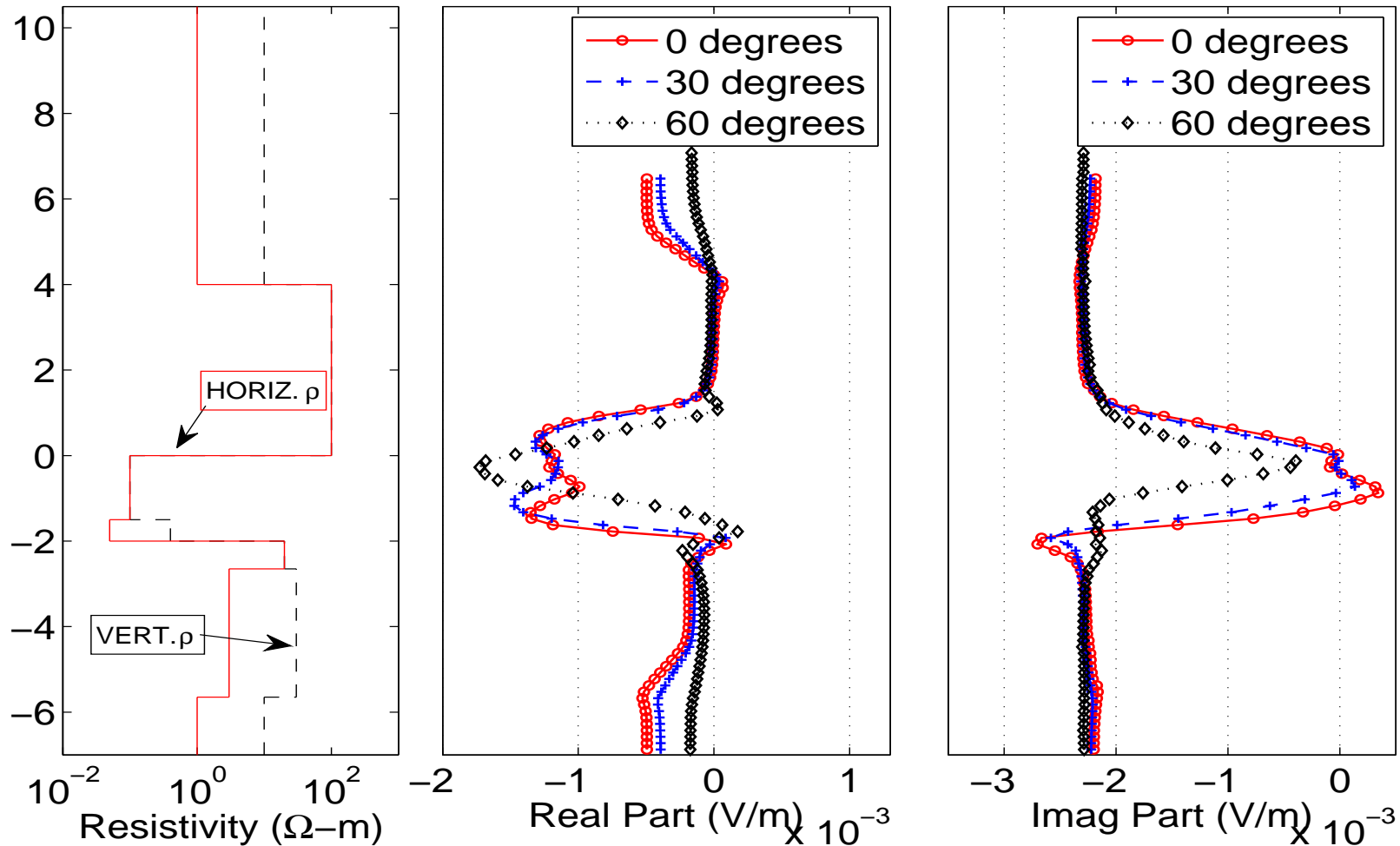
Wireline, 150 Khz



# NUMERICAL RESULTS: AC RESULTS

## Dip Angle + Anisotropy

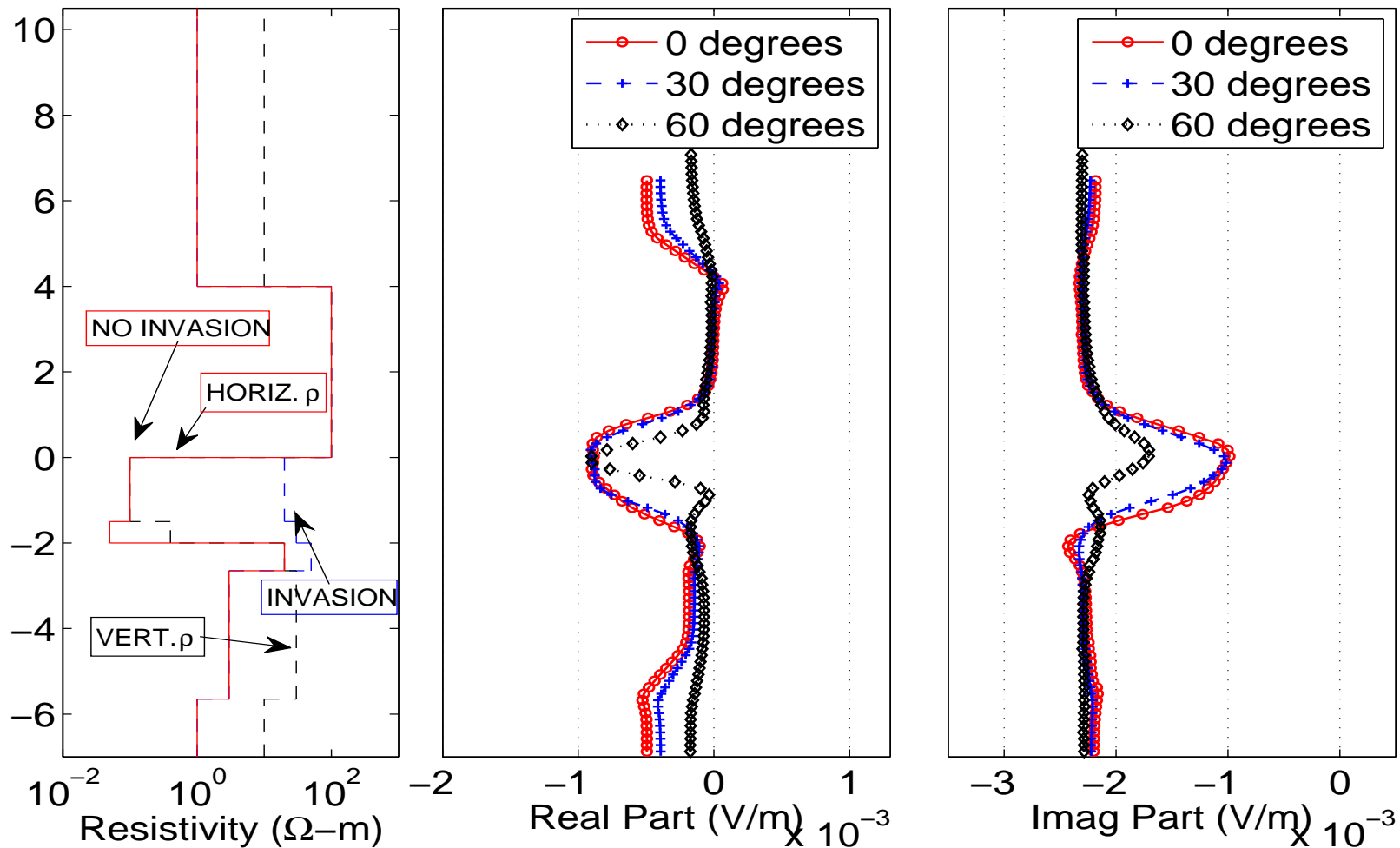
Wireline, 150 Khz



# NUMERICAL RESULTS: AC RESULTS

## Dip Angle + Invasion + Anisotropy

Wireline, 150 Khz

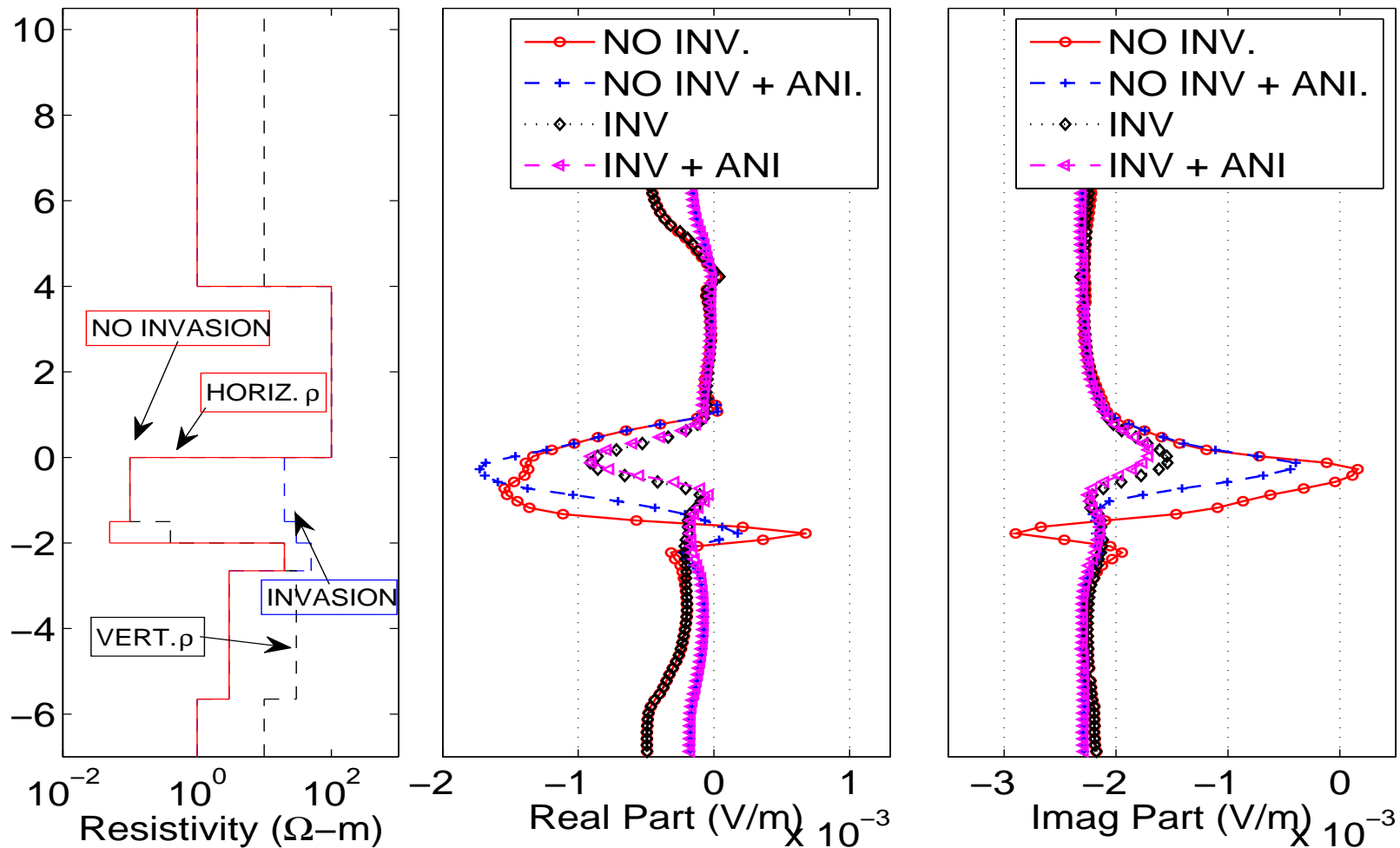




# NUMERICAL RESULTS: AC RESULTS

## 60-Degree Deviated Well

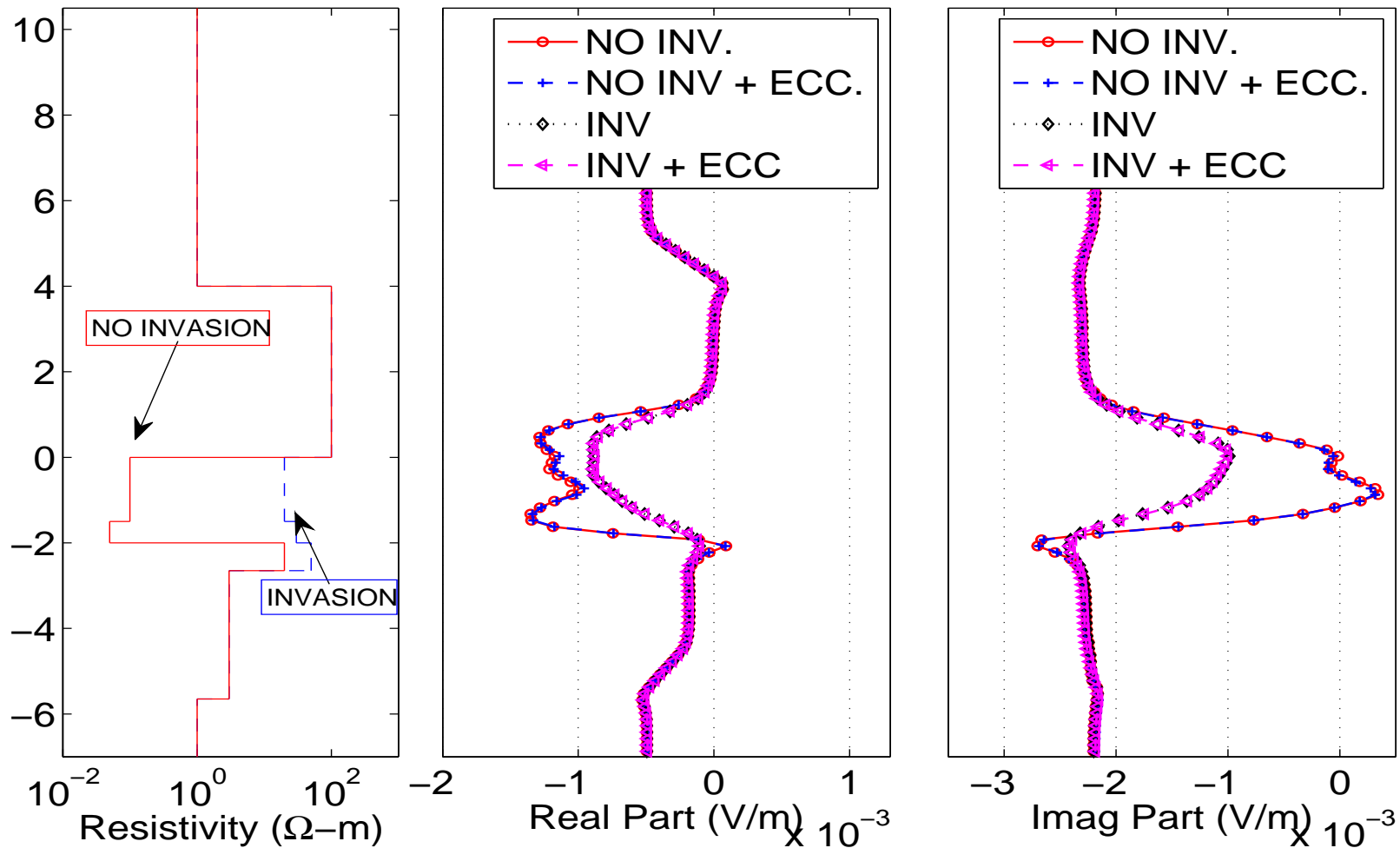
Wireline, 150 Khz



# NUMERICAL RESULTS: AC RESULTS

## Vertical Well with 0.03 m Eccentricity

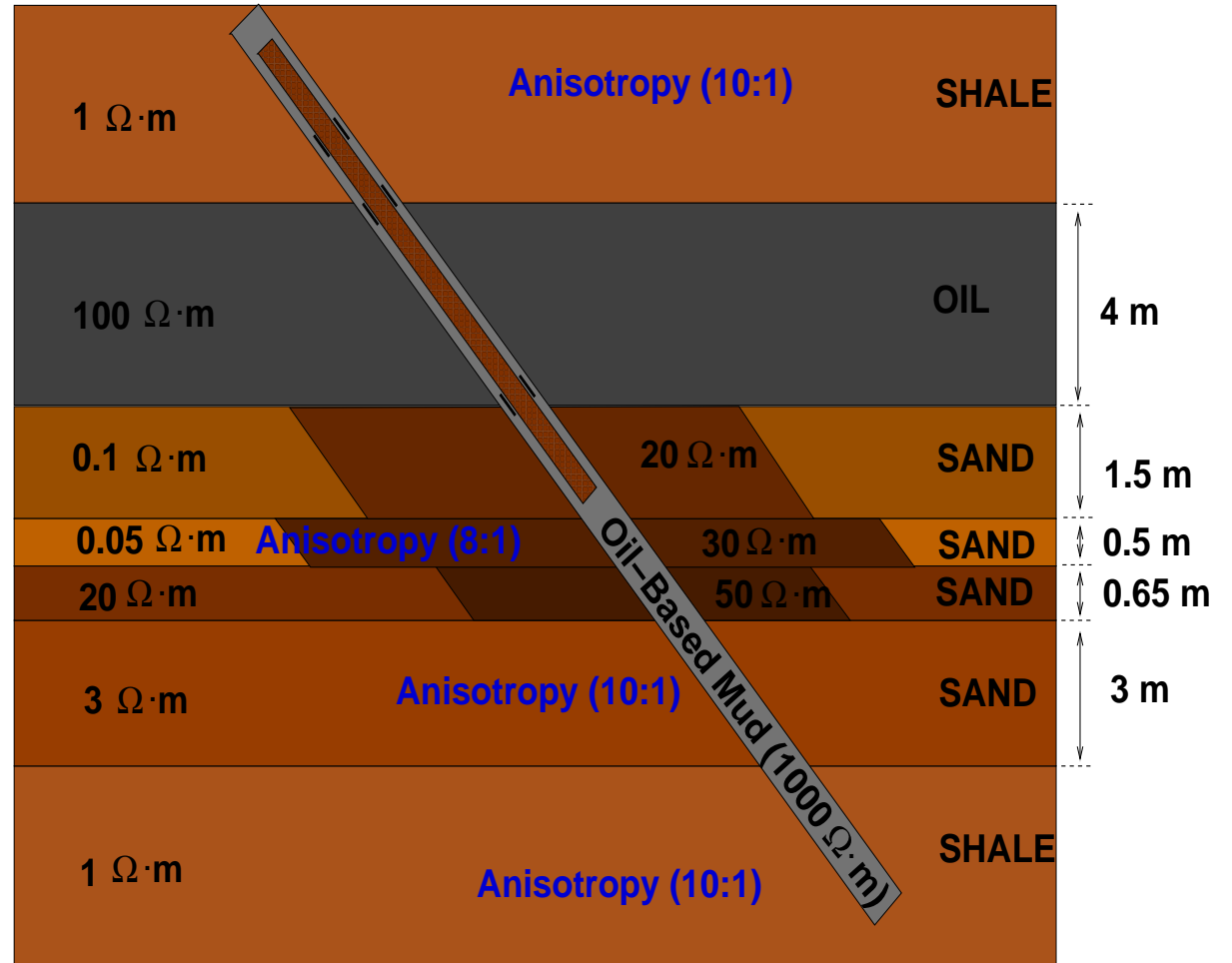
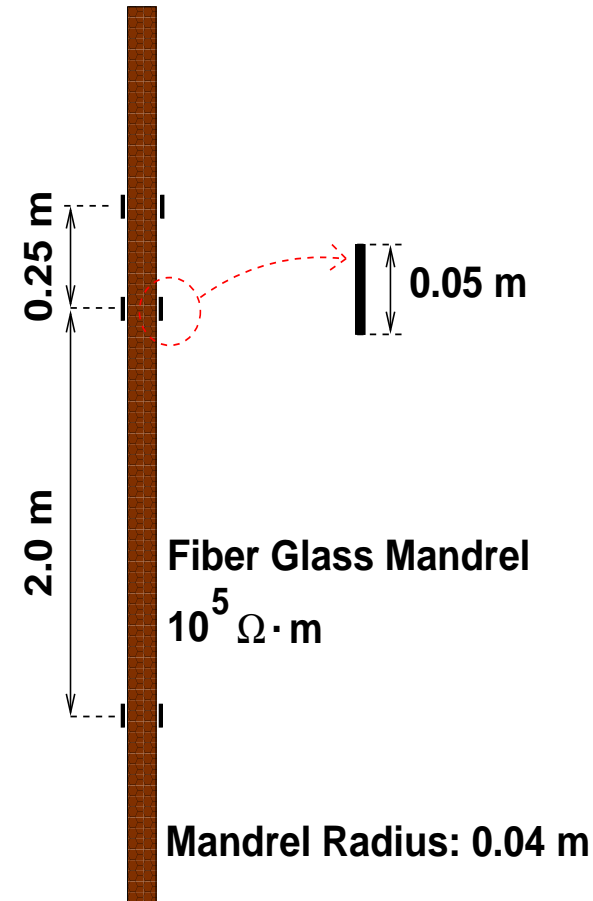
Wireline, 150 Khz



# NUMERICAL RESULTS: AC RESULTS

## Model Problem

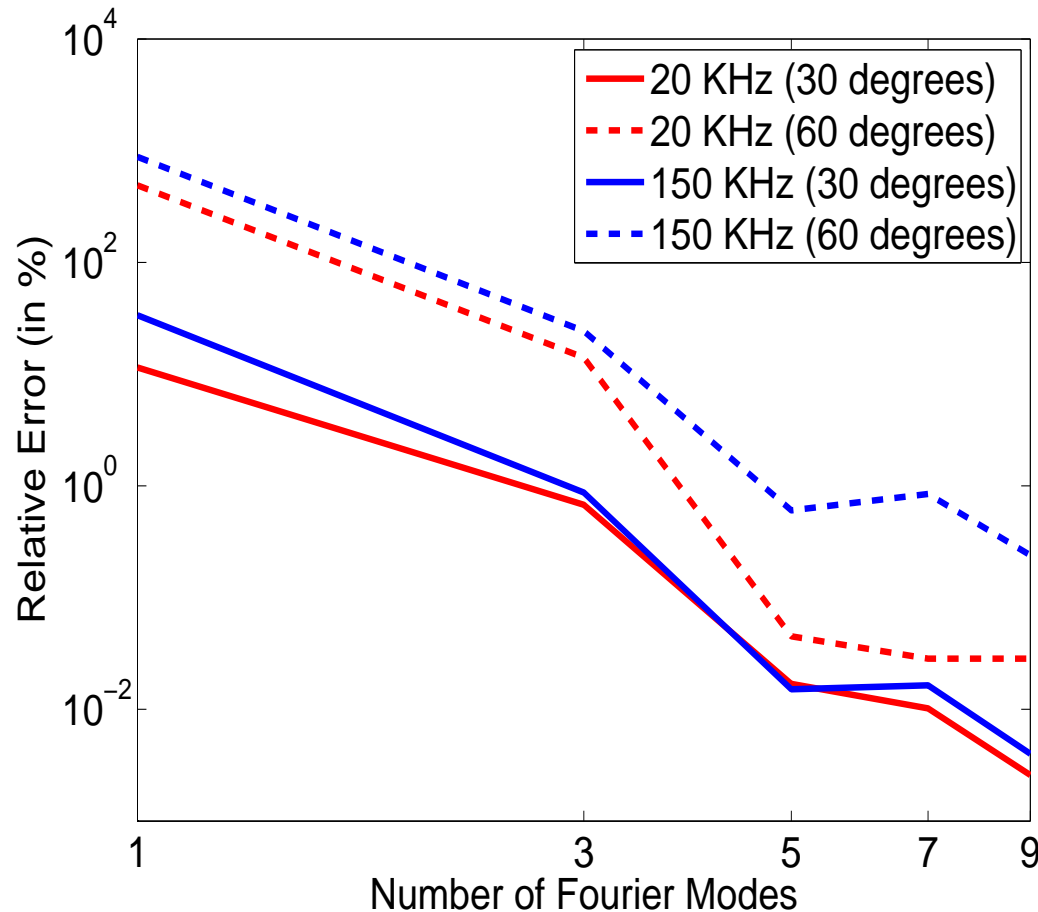
20 kHz (Wireline)



# NUMERICAL RESULTS: AC RESULTS

## Verification

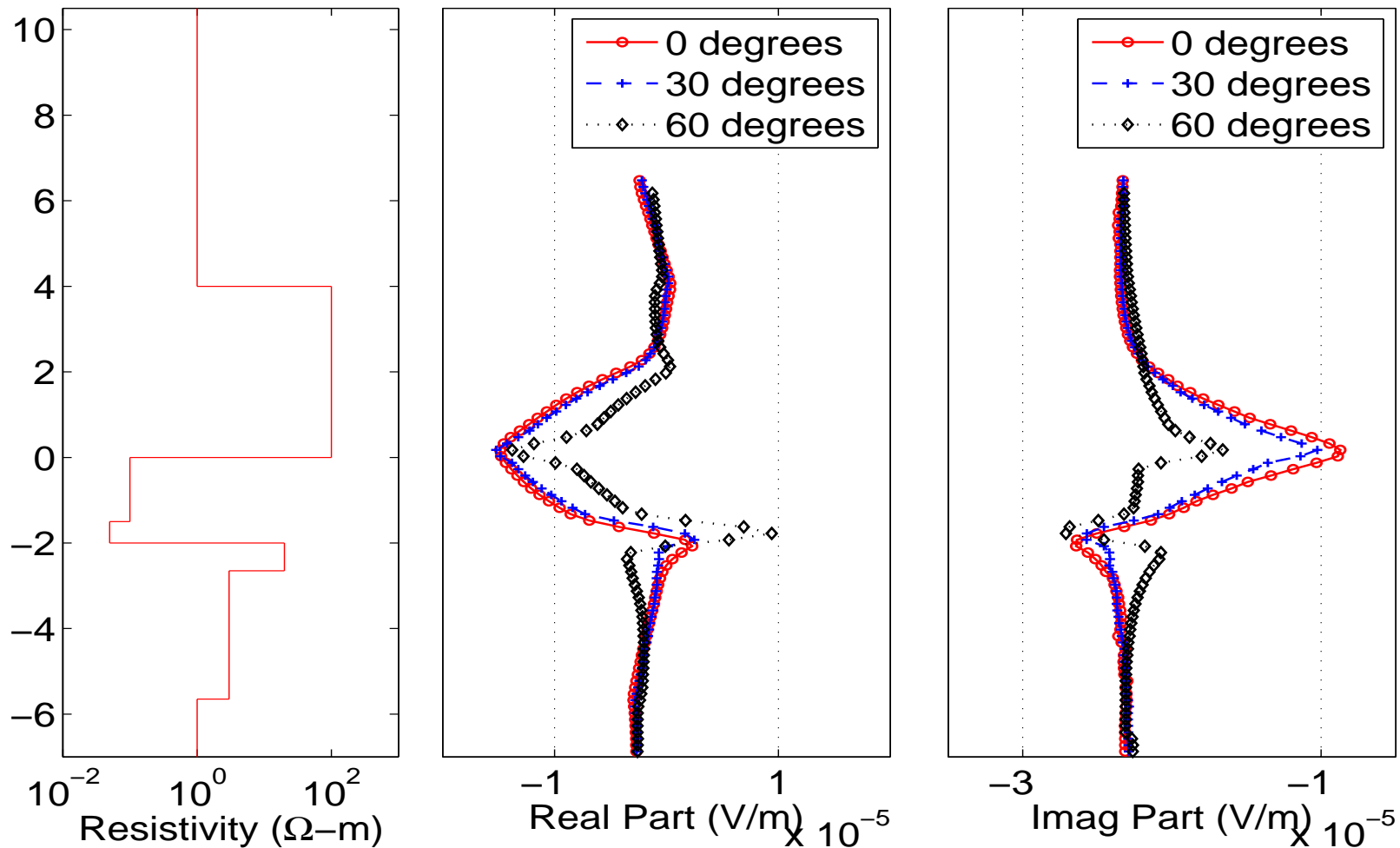
### Logging Instrument in a Homogeneous Formation



# NUMERICAL RESULTS: AC RESULTS

## Dip Angle

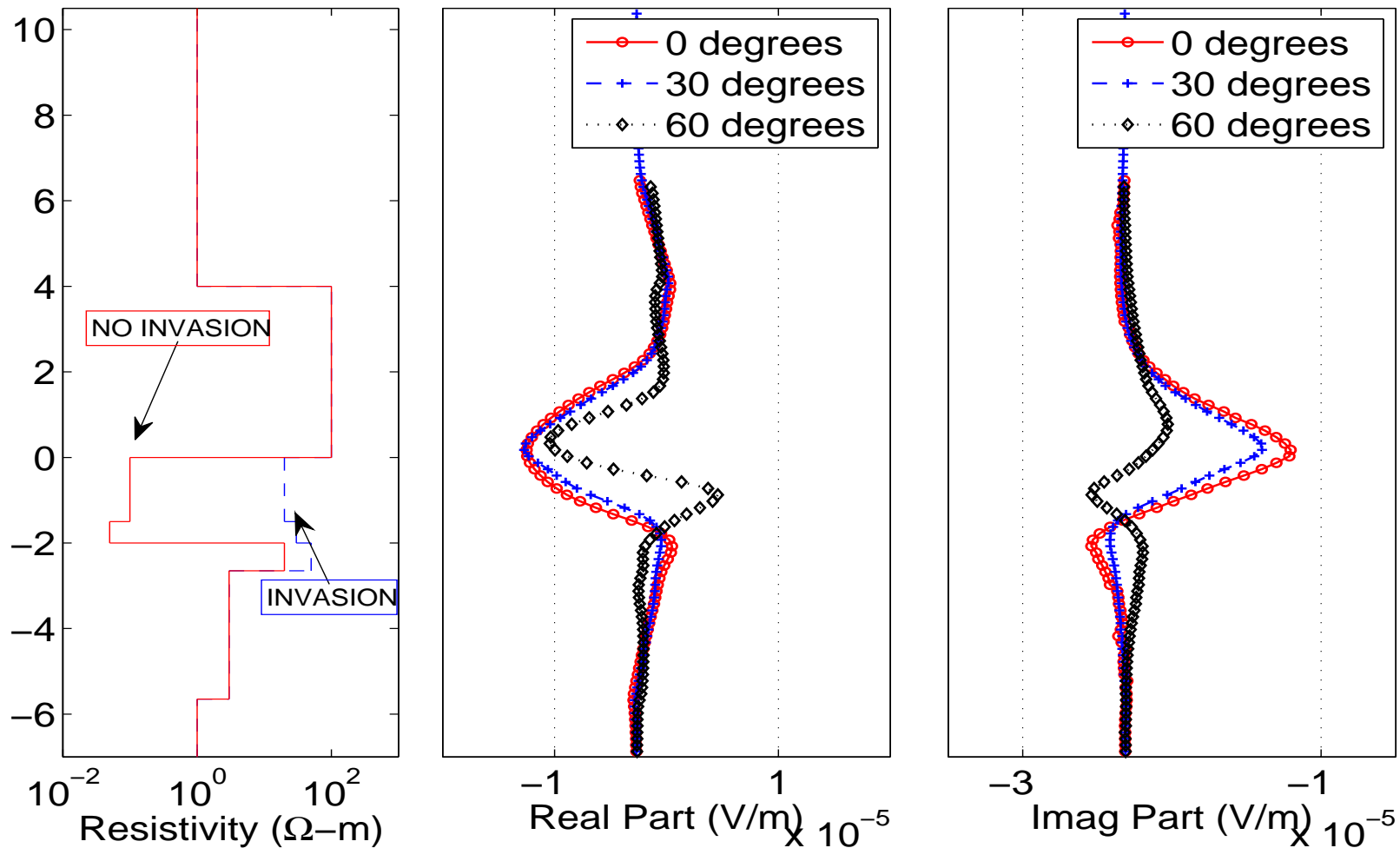
Wireline, 20 Khz.



# NUMERICAL RESULTS: AC RESULTS

## Dip Angle + Invasion

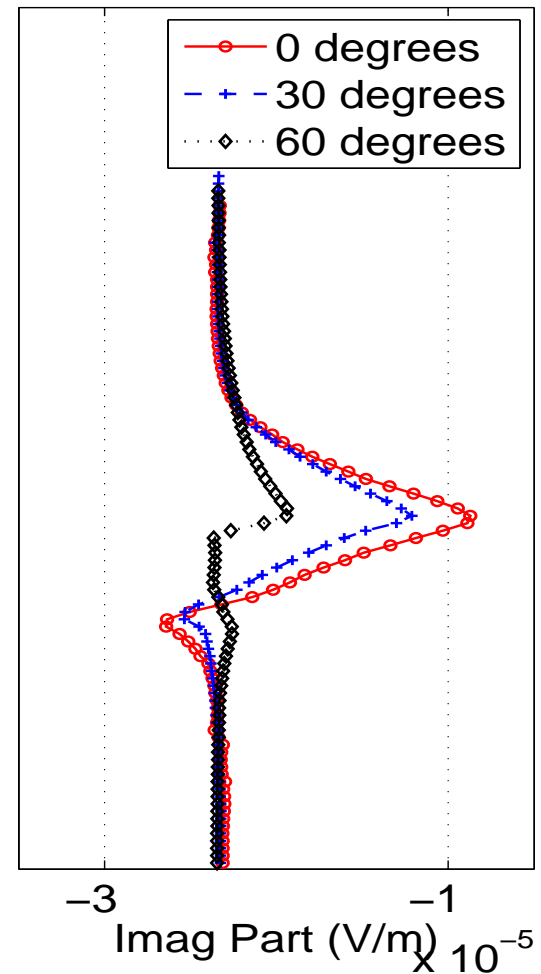
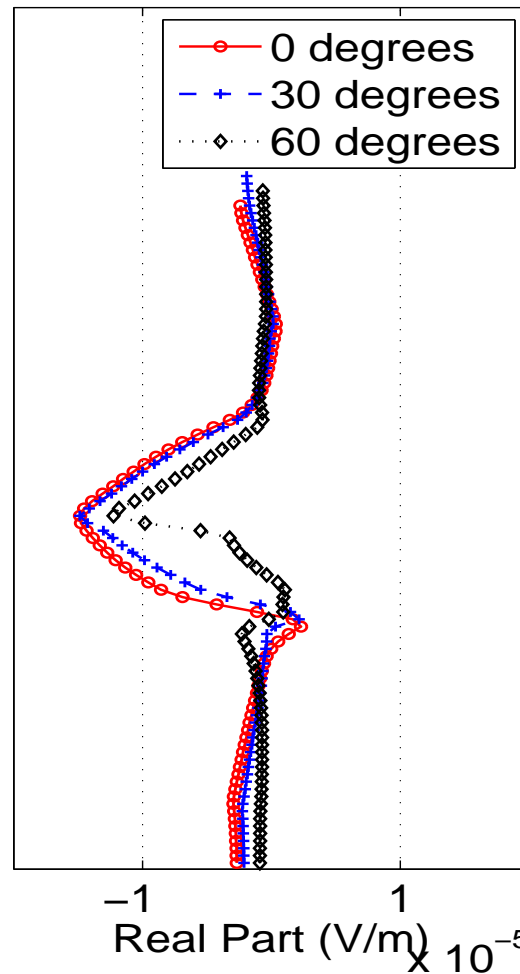
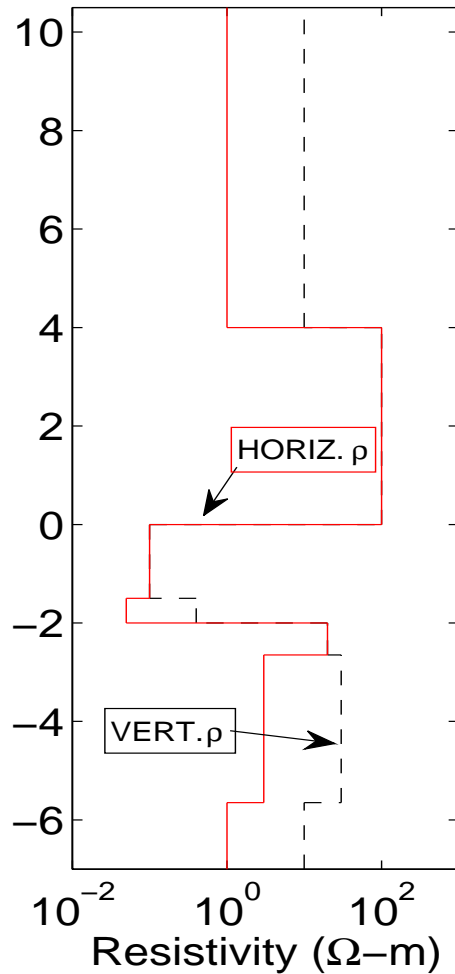
Wireline, 20 Khz.



# NUMERICAL RESULTS: AC RESULTS

## Dip Angle + Anisotropy

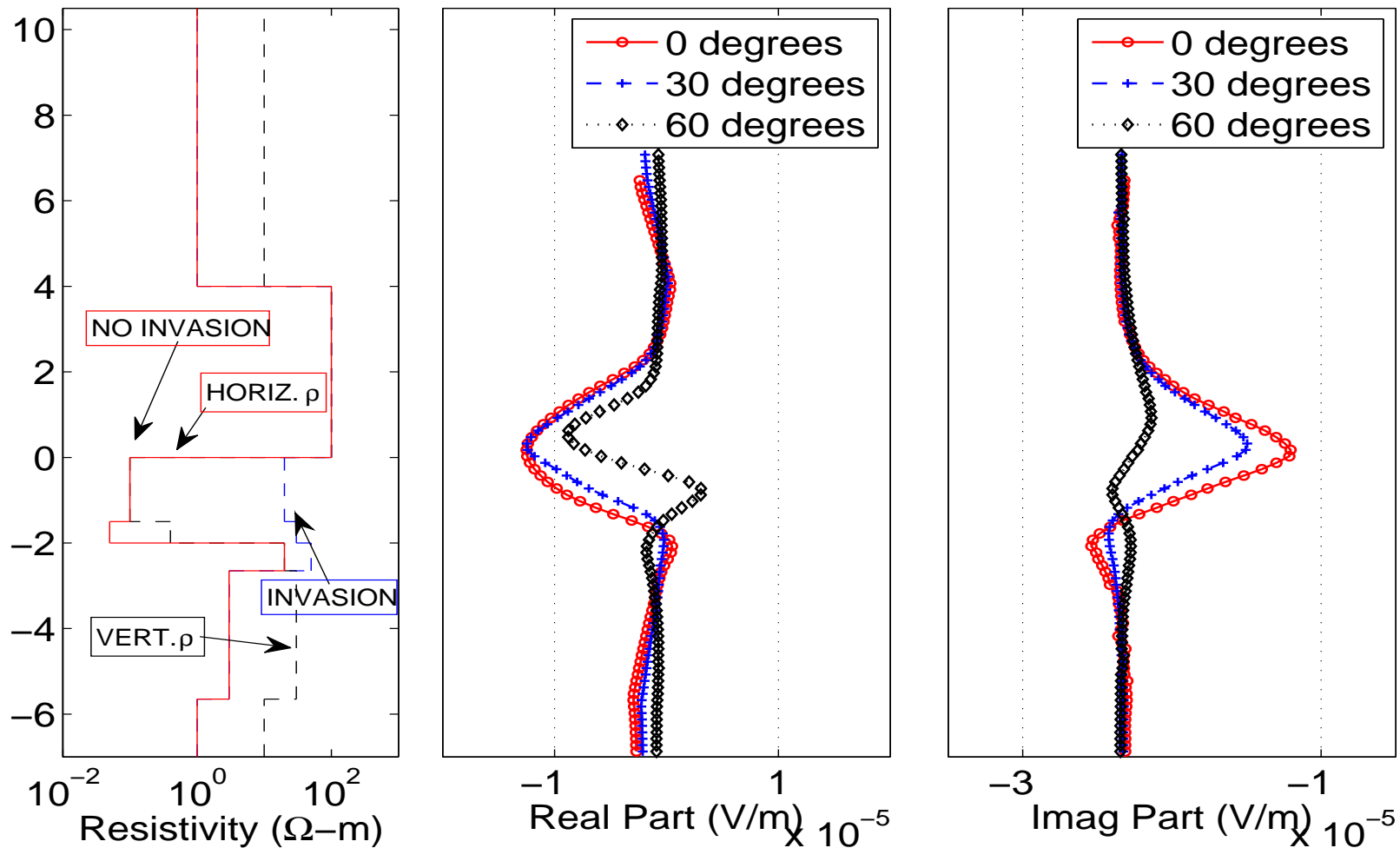
Wireline, 20 Khz.



# NUMERICAL RESULTS: AC RESULTS

## Dip Angle + Invasion + Anisotropy

Wireline, 20 Khz.

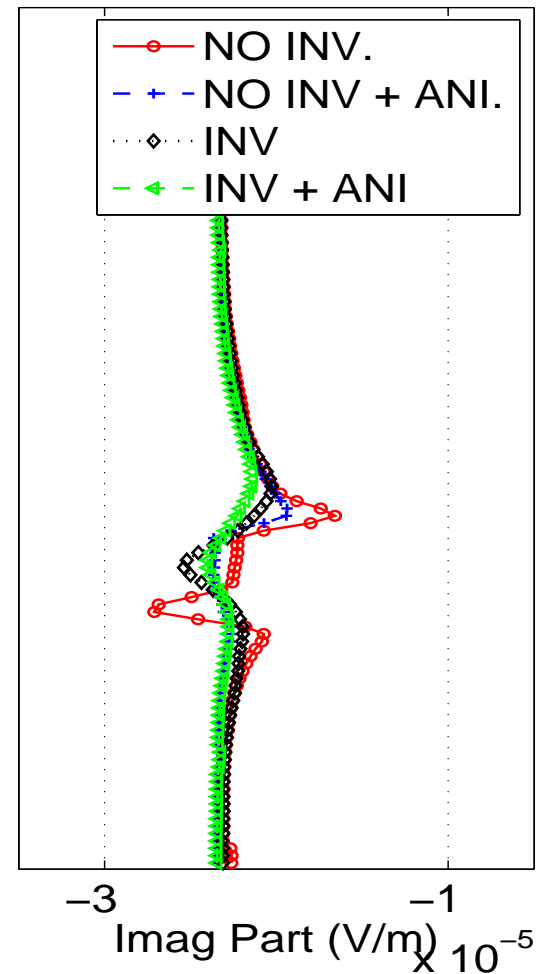
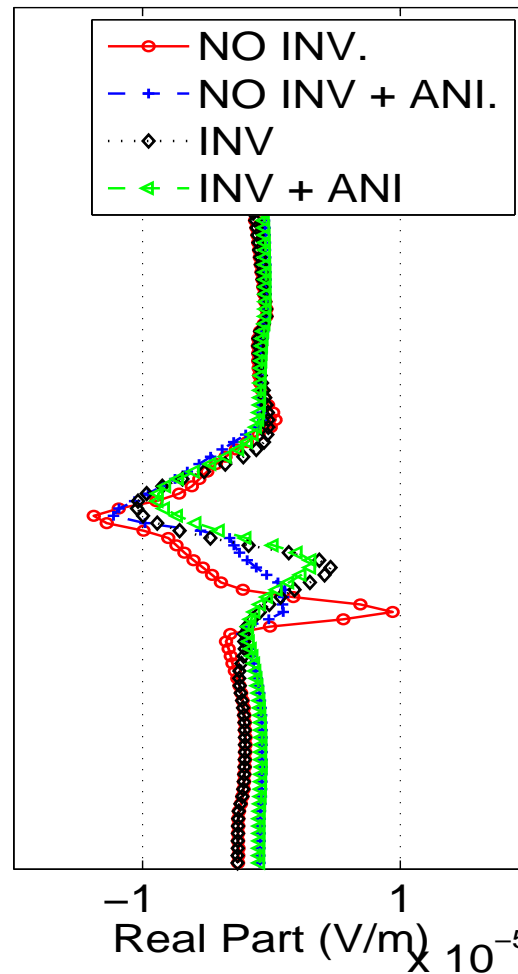
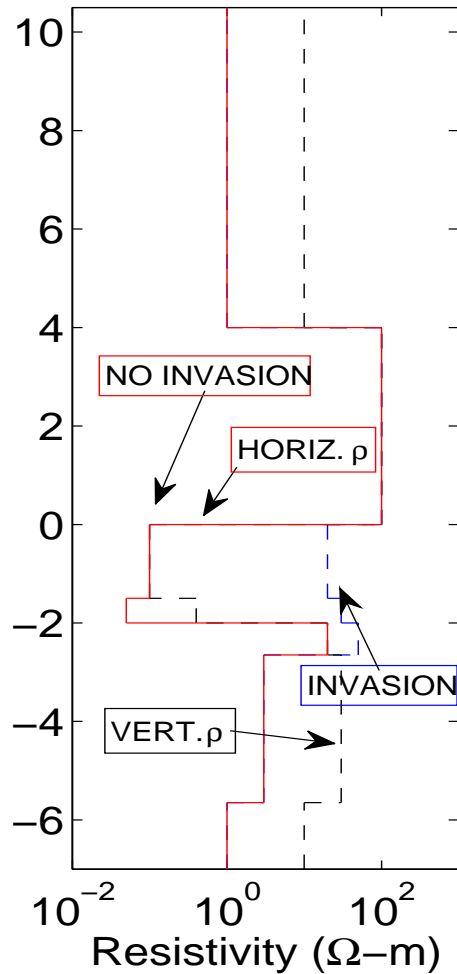




# NUMERICAL RESULTS: AC RESULTS

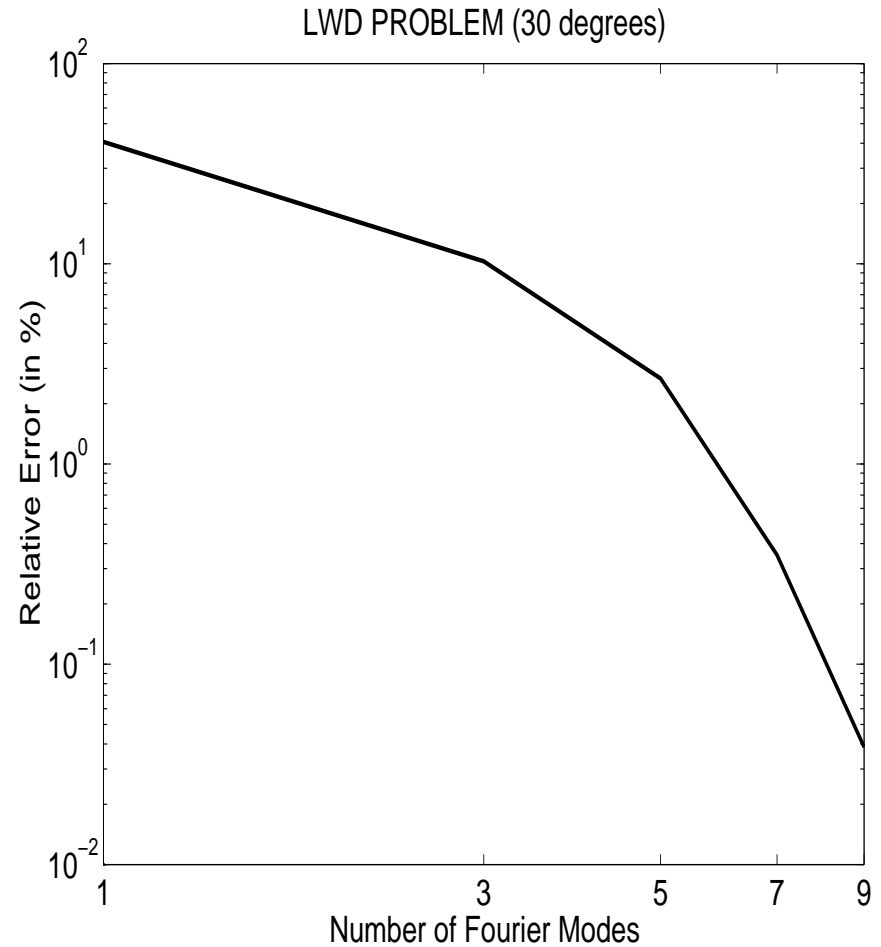
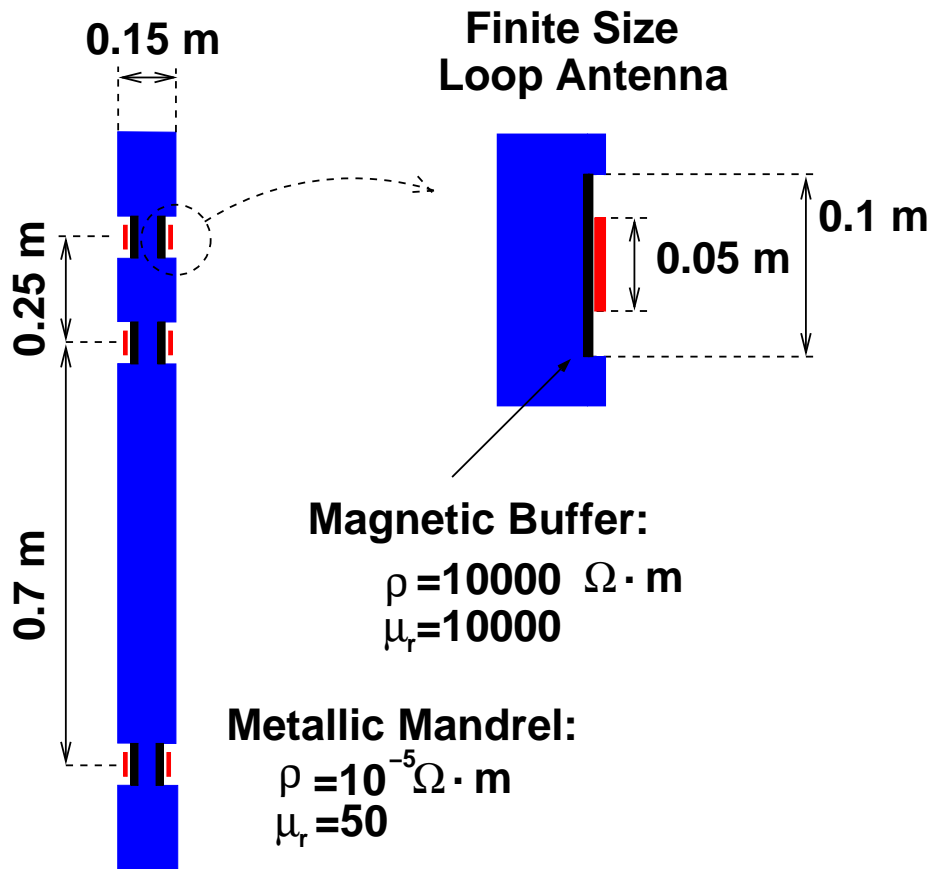
## 60-Degree Deviated Well

Wireline, 20 Khz.



# NUMERICAL RESULTS: LWD

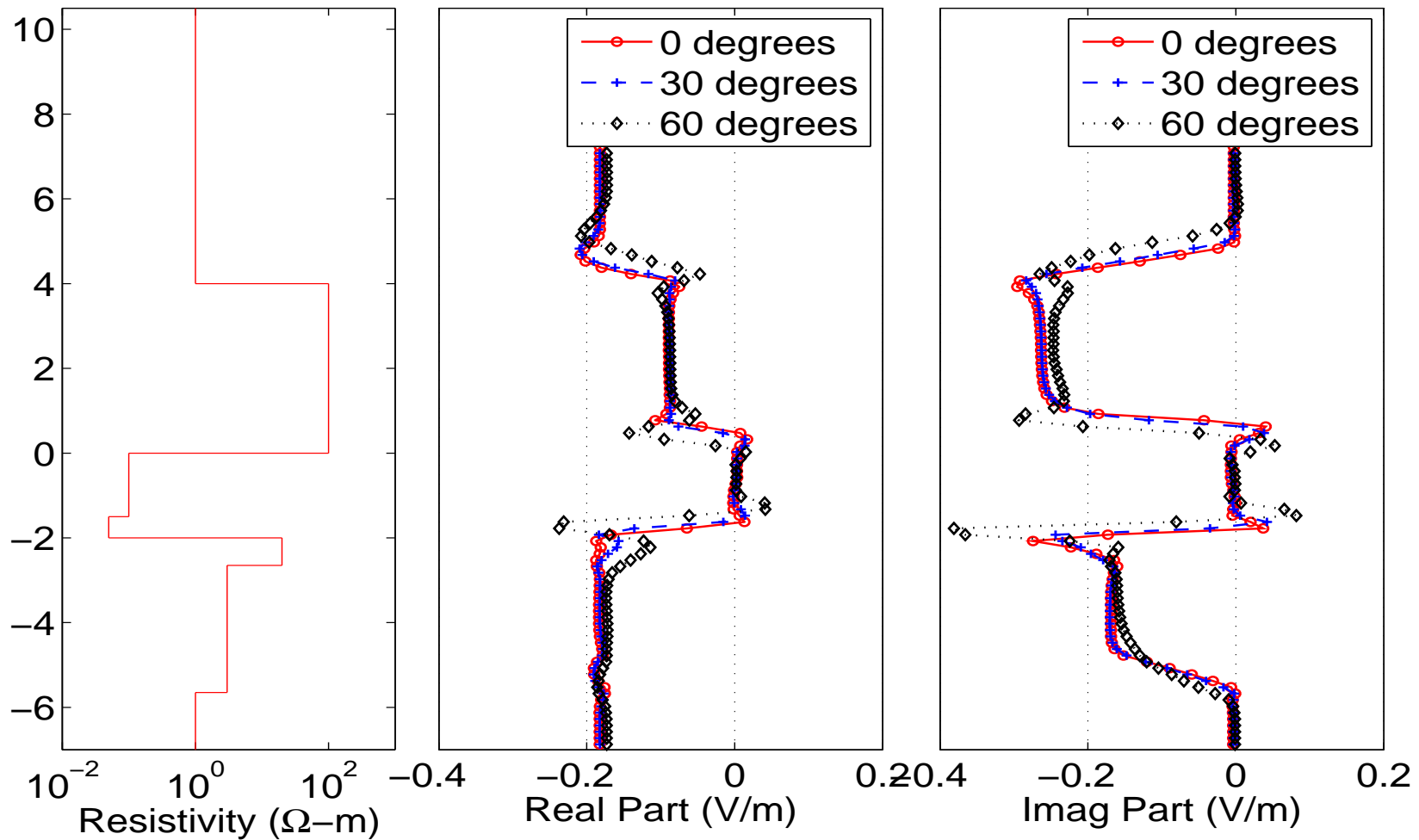
## Model Problem and Verification



# NUMERICAL RESULTS: LWD

## Dip Angle

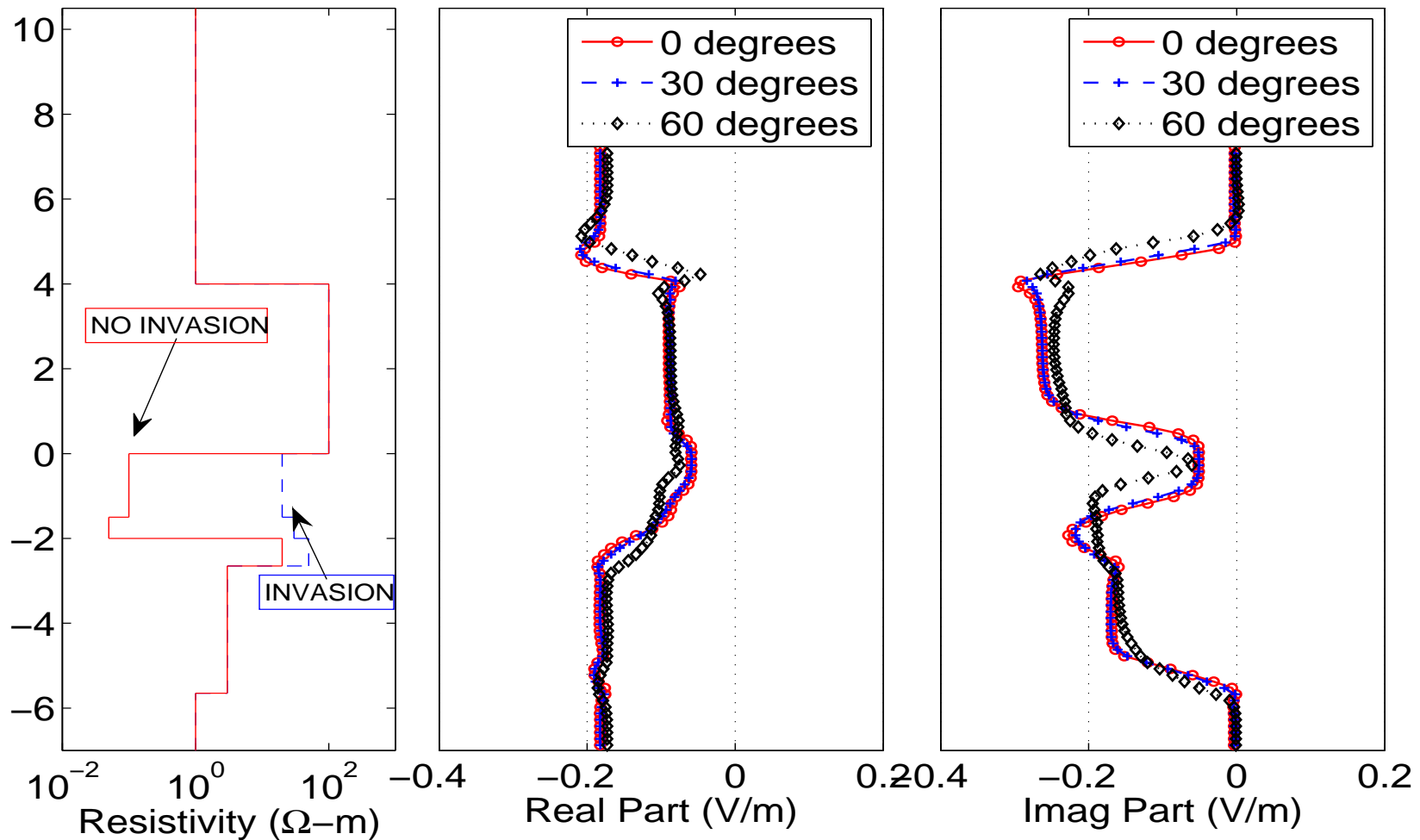
LWD, 2 Mhz



# NUMERICAL RESULTS: LWD

## Dip Angle + Invasion

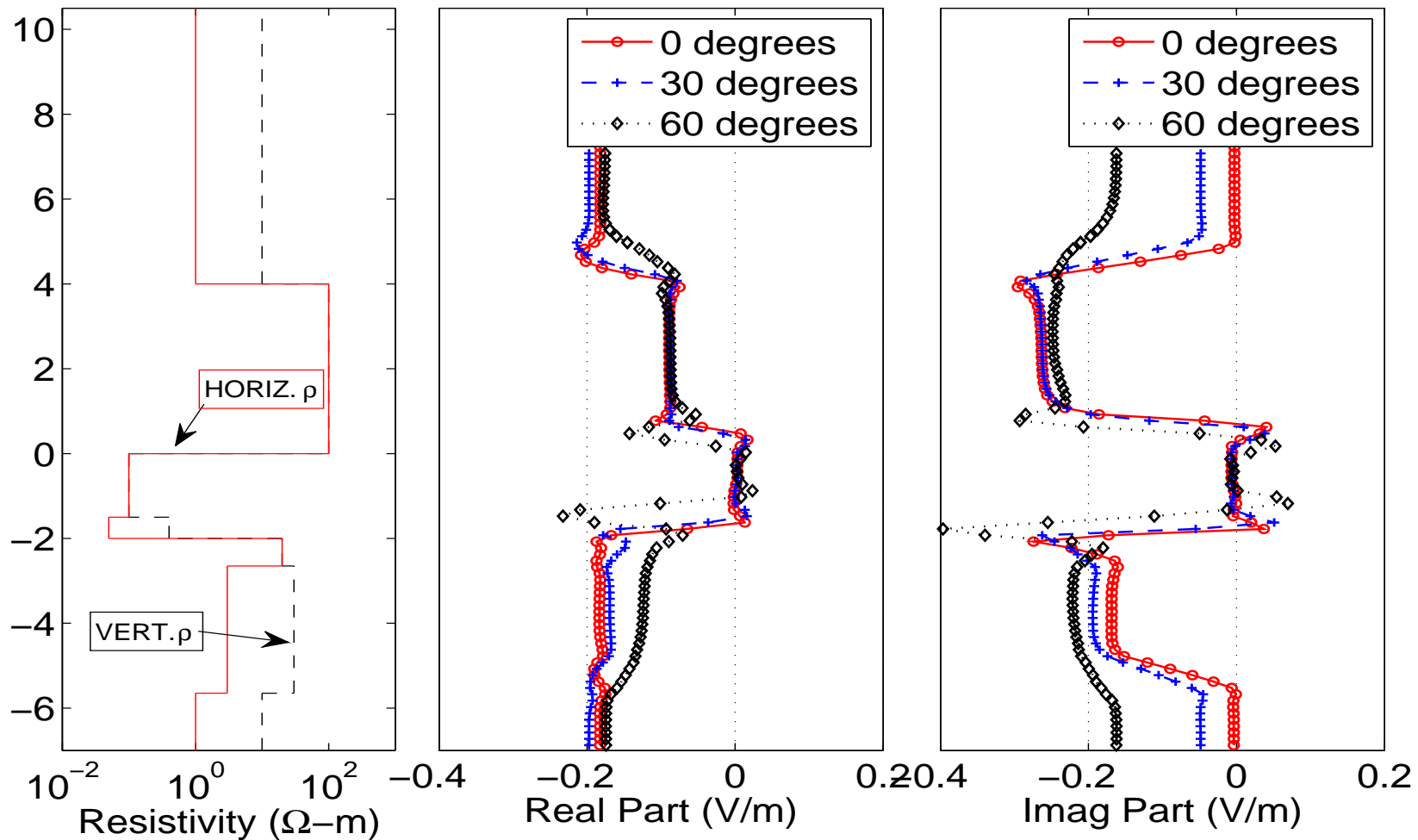
LWD, 2 Mhz



# NUMERICAL RESULTS: LWD

## Dip Angle + Anisotropy

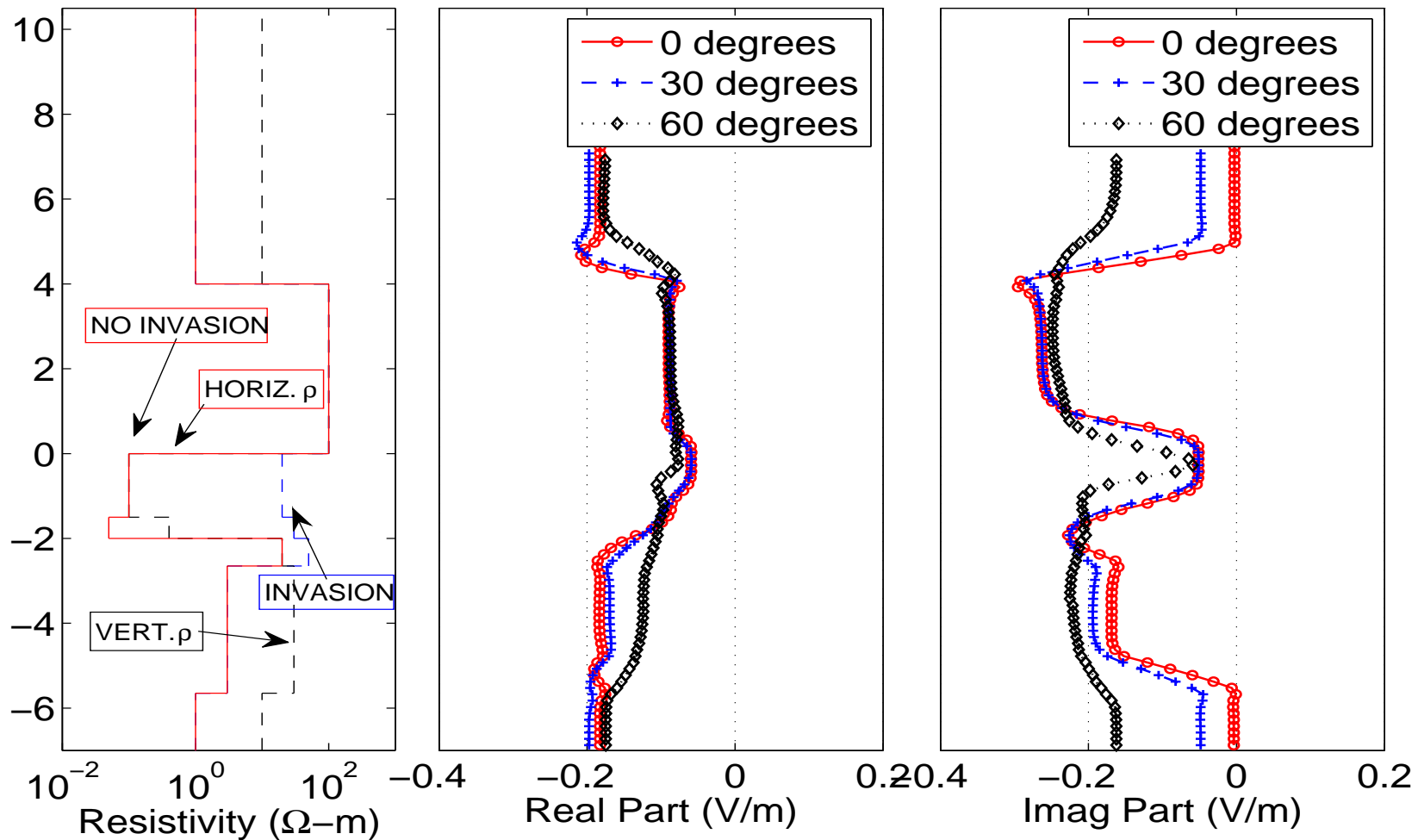
LWD, 2 Mhz



# NUMERICAL RESULTS: LWD

## Dip Angle + Invasion + Anisotropy

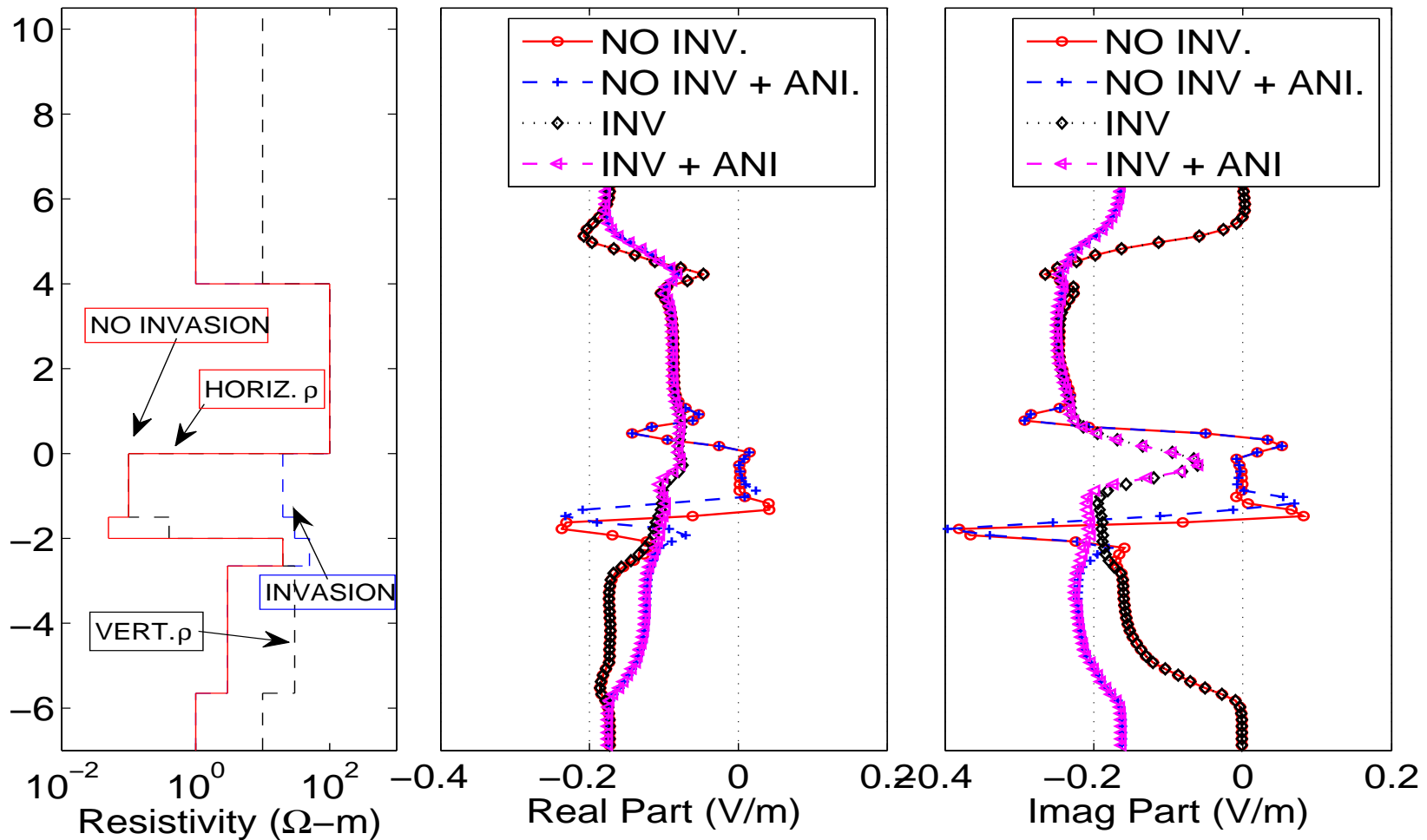
LWD, 2 Mhz



# NUMERICAL RESULTS: LWD

## 60-Degree Deviated Well

LWD, 2 Mhz



## CONCLUSIONS AND FUTURE WORK

---

**We have developed a new method based on a Fourier series expansion in a non-orthogonal system of coordinates.**

- **LIMITATION:** Geometry of the problem.
- **ADVANTAGE:** It combines exponential convergence with sparse (penta-diagonal) matrices.
- **FURTHER APPLICABILITY OF THE METHOD:**
  - Eccentric measurements and tilted antennas.
  - **Time-domain simulations.**
  - **Multi-Physics:** Resistivity logging instruments, sonic logging instruments (acoustics + elasticity), fluid-flow, geomechanics, etc.
  - **Inverse problems.**
- **FUTURE WORK:** Iterative solver based on 2D-block Jacobi preconditioners.

---

Department of Petroleum and Geosystems Engineering



# ACKNOWLEDGMENTS

## Sponsors of UT Consortium on Formation Evaluation

